Atomic Resolution Electron Tomography

Jianwei (John) Miao

Dept. of Physics & Astronomy and California NanoSystems Institute
University of California, Los Angeles

14ème Colloque Sfμ 2015

Nice, France, June 30 – July 3

Methods for Visualizing Atomic Structure

- X-ray crystallography can reveal the *globally*-averaged 3D atomic structure of crystals.

- Transmission electron microscopes can resolve atoms in 2D projections of 3D samples.

- Scanning tunneling and atom force microscopes can image atomic structure at surface.

Richard Feynman stated in 1959: “It would be very easy to make an analysis of any complicated chemical substance; all one would have to do would be to look at it and see where the atoms are... I put this out as a challenge: Is there no way to make the electron microscope more powerful?”

A general imaging method that can determine the 3D positions of individual atoms in matter would have revolutionary impact in modern science and technology.

Why Tomography?

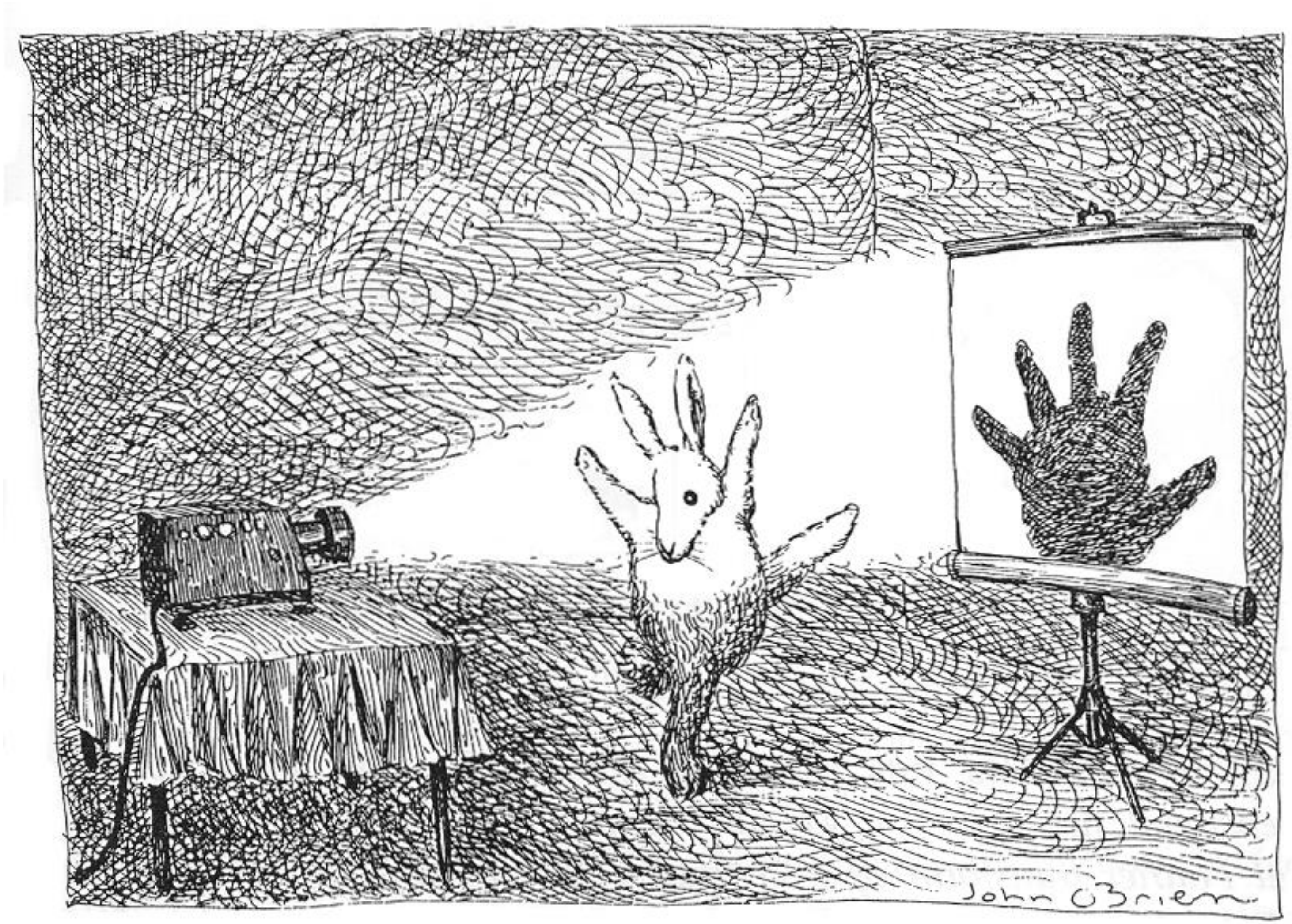

A single projection is usually insufficient to infer the structure of a general 3D object.
(New Yorkers Magazine, 1991)

Conventional Tomographic Reconstruction Method: Weighted (Filtered) Back Propagation (WBP, FBP)

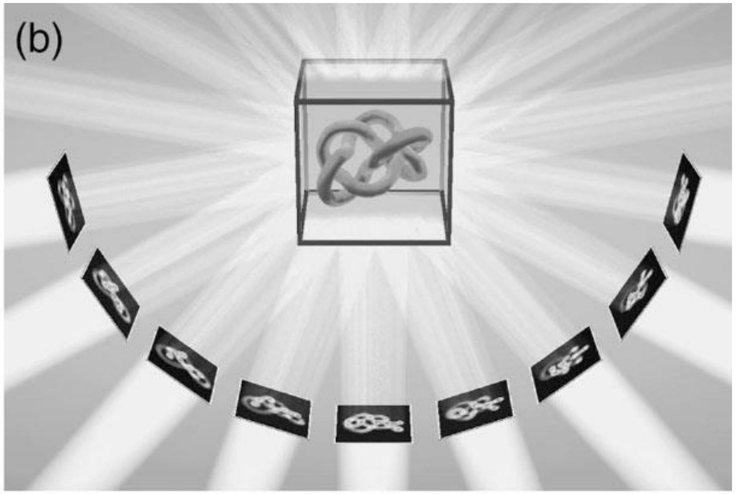

The missing wedge

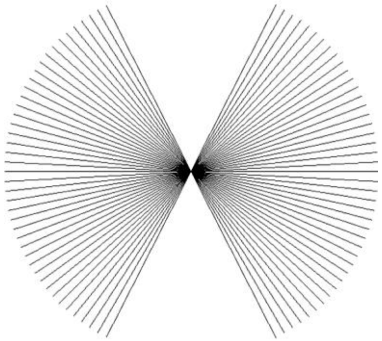

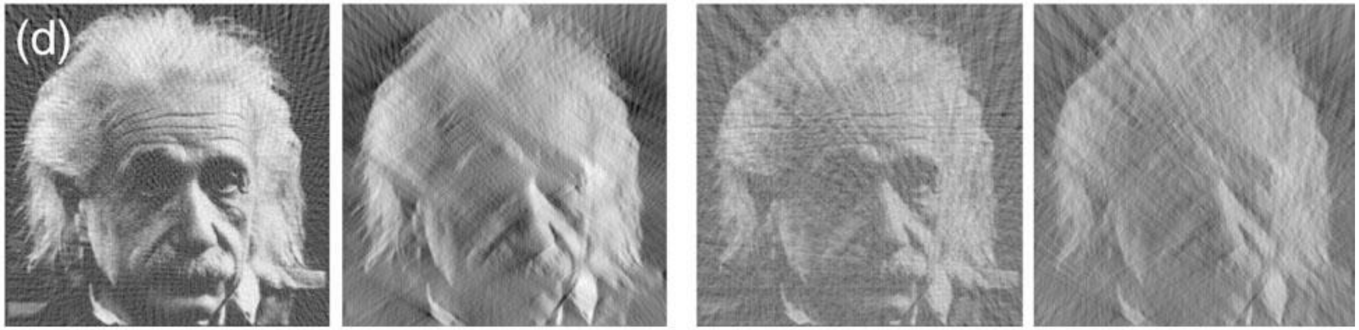

91 projections | **61 projections (with a missing wedge)** | **37 projections** | **25 projections**

Baumeister *et al.*, *Trends Cell Biol.* **9**, 81 (1999).

STEM Tomography for Materials (~1 nm^3 Resolution)

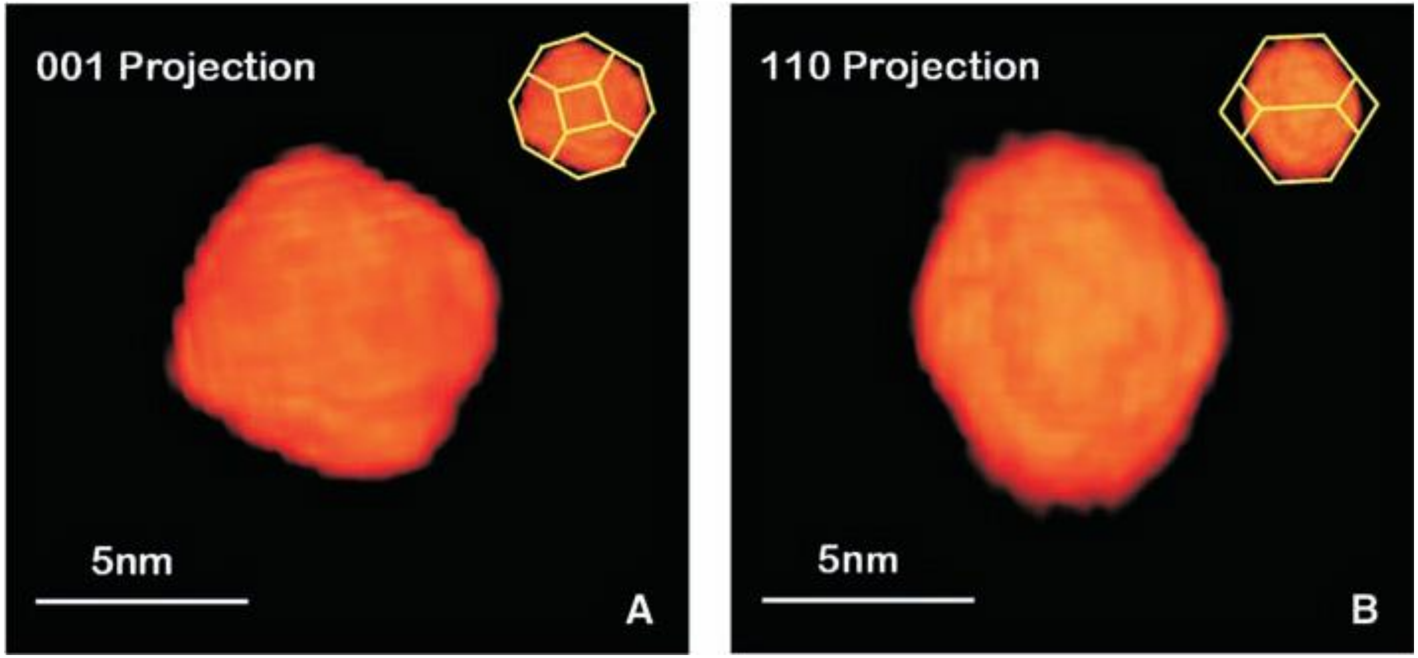

Arslan, Yates, Browning, Midgley, *Science* **309**, 2195 (2005).

Limitations for achieving atomic resolution:

(i) Aligning the projections with atomic precision is challenging .

(ii) Dynamical scattering and non-linear effects in electron microscopy.

(iii) Radiation damage limits the number of projections measurable from an object.

(iv) Specimens cannot usually be tilted beyond ±79° (a missing wedge).

Projection Misalignment in Tomographic Tilt Series

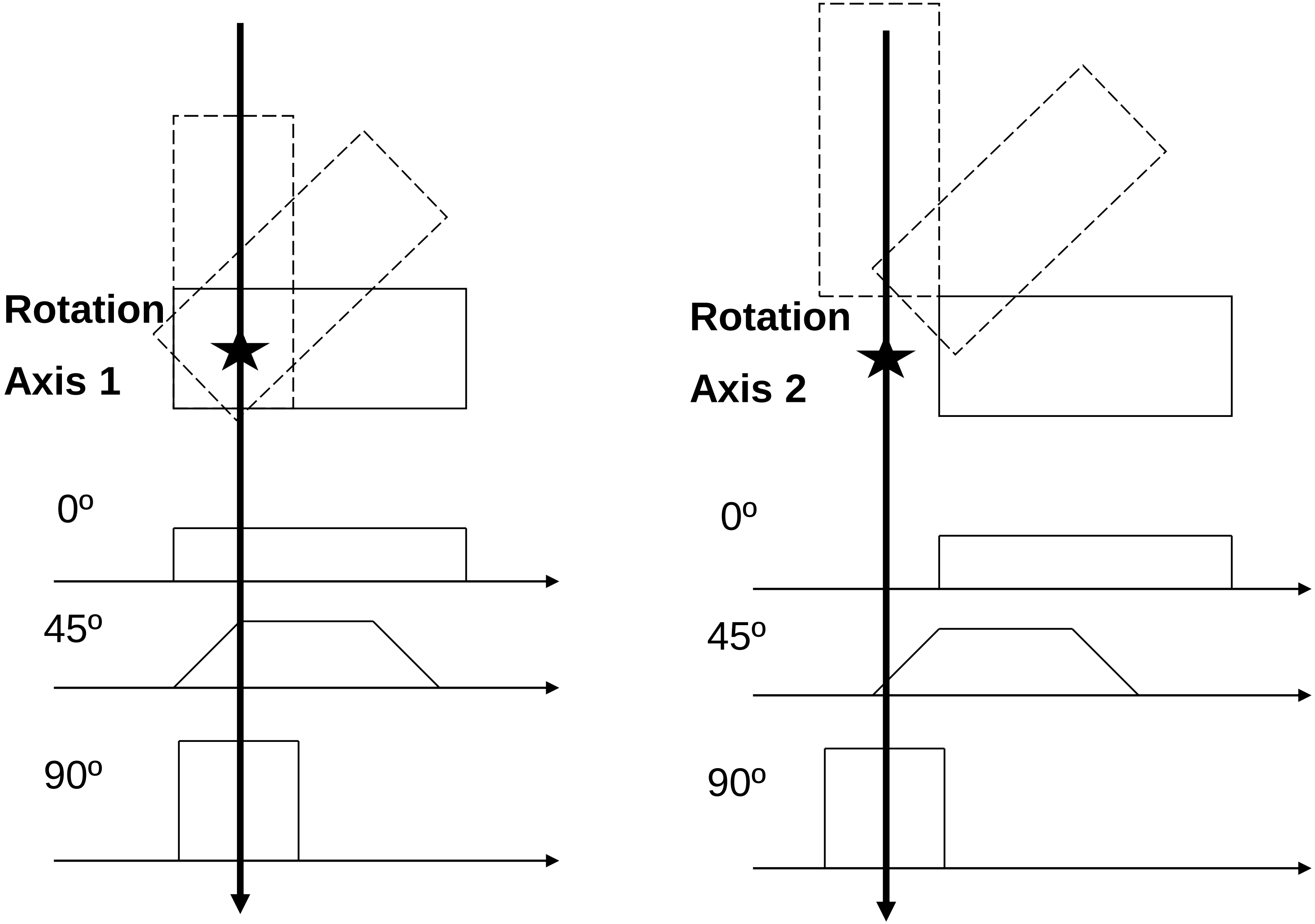

Achieving Atomic Precision Alignment with the Center of Mass (CM) Method

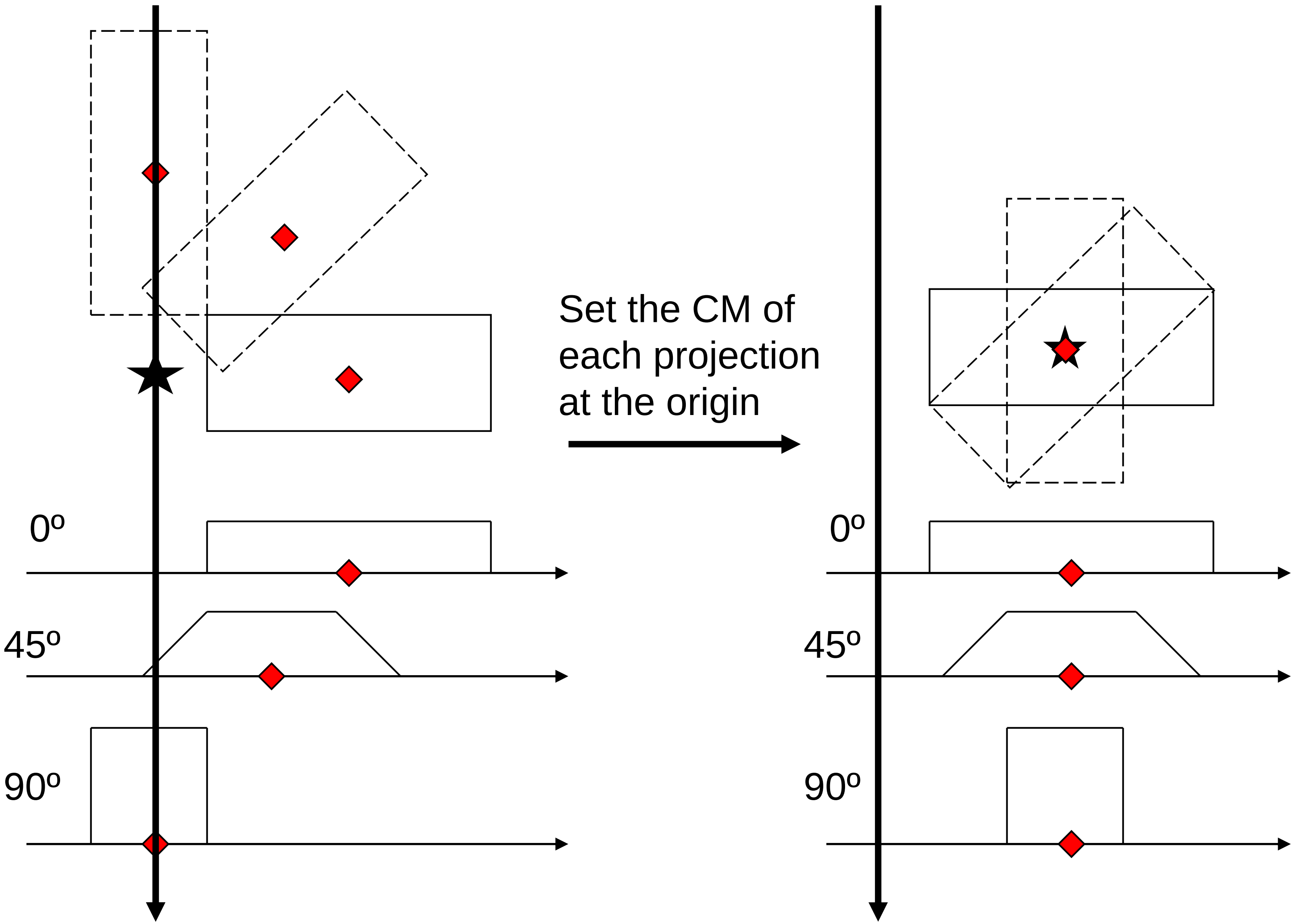

The Pseudopolar Fast Fourier Transform (PPFFT)

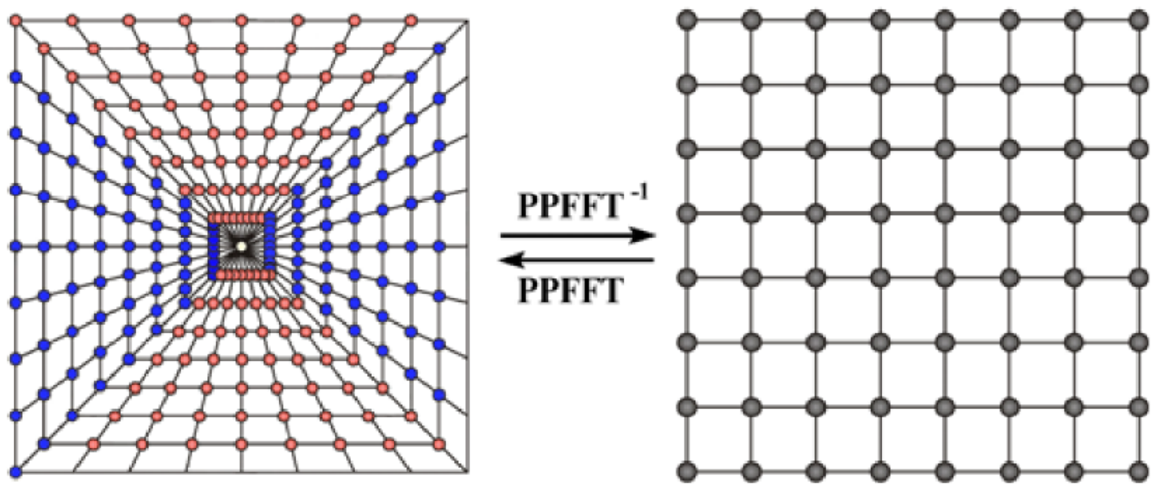

An exact, invertible pseudopolar fast Fourier transform between the Cartesian and pseudopolar grid has been developed.

The lines are equally sloped ($\Delta \tan\theta$) instead of equally angled ($\Delta\theta$).

Mersereau, Oppenheim, *Proc. IEEE* **62** 1319 (1974).
Averbuch, Coifman, Donoho, Israeli, Shkolnisky, *SIAM J. Sci. Comput*. **30**, 764 (2008).

Equal Slope Tomography (EST)

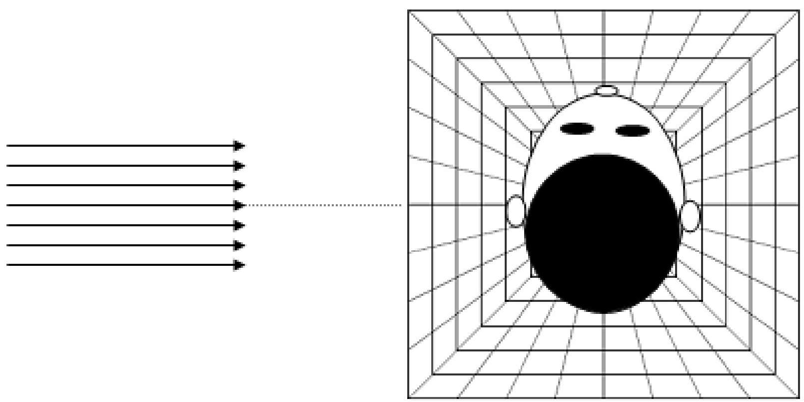

Equally Sloped Tomography

$$y = s_x x$$

$$\Delta s_x = \frac{1}{4}$$

$$\Delta\theta = 14.0^{\circ}$$

Miao, Förster, Levi, *PRB* **72**, 052103 (2005).

The Iterative EST Method

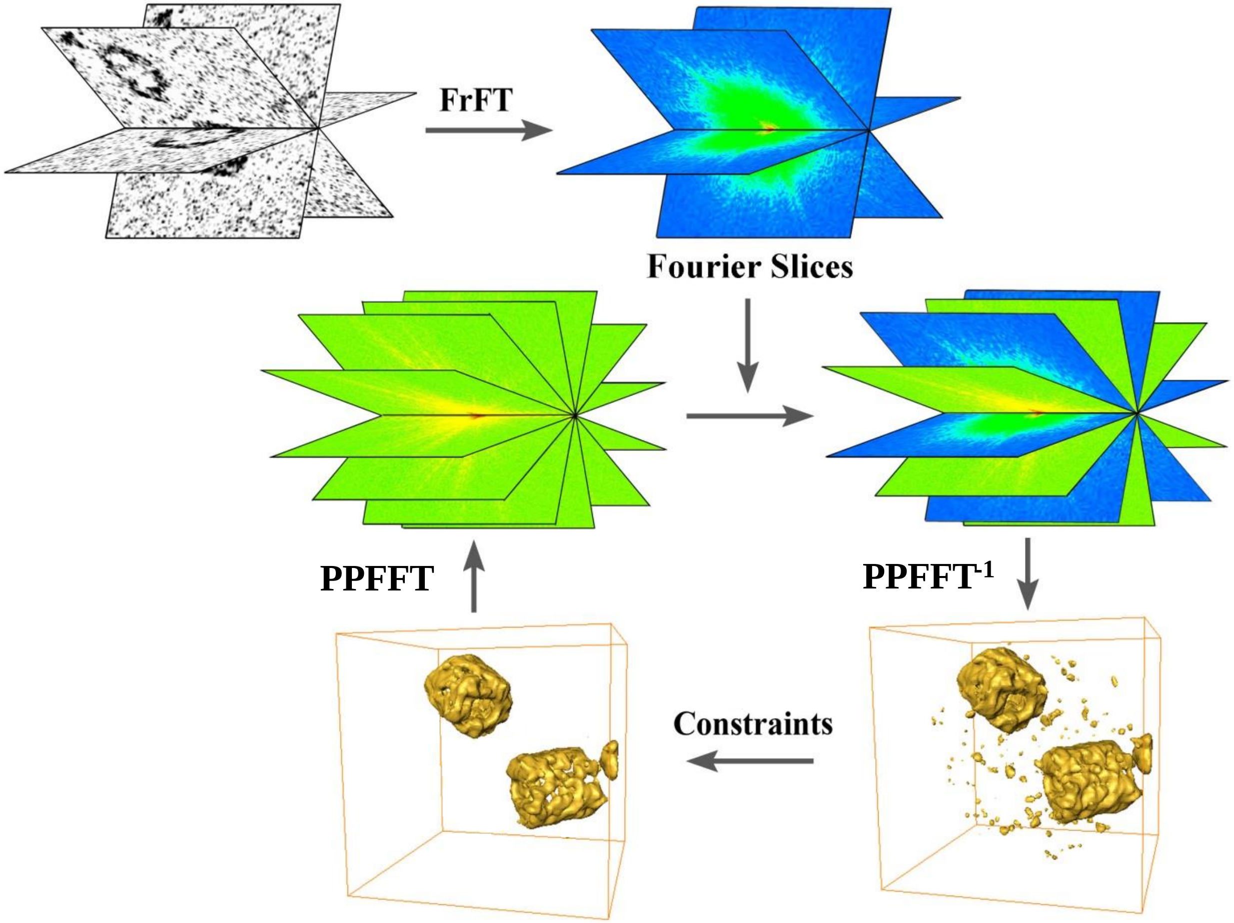

Miao, Förster, Levi, *PRB*. **72**, 052103 (2005).
Lee *et al*., *J. Struct. Biol*. **164**, 221 (2008).
Mao, Fahamian, Osher, Miao, *IEEE Trans. Image Processing* **19**, 1259 (2010).
Free EST software and code: www.physics.ucla.edu/research/imaging/EST

Experimental STEM Tilt Series of 69 Projections Acquired from a 10 nm Au Particle

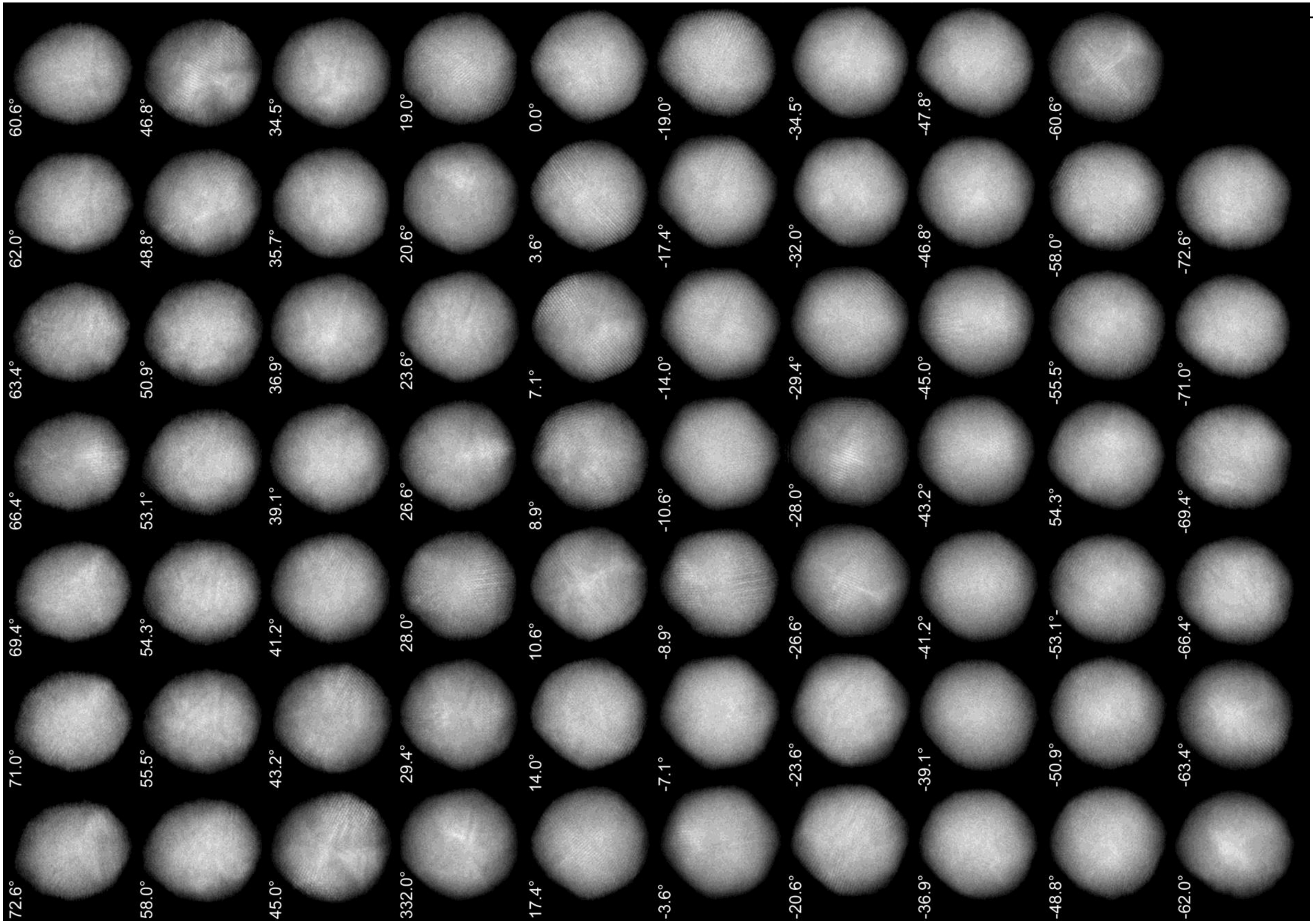

Three 0° Projections Measured during the Acquisition of the Tilt Series

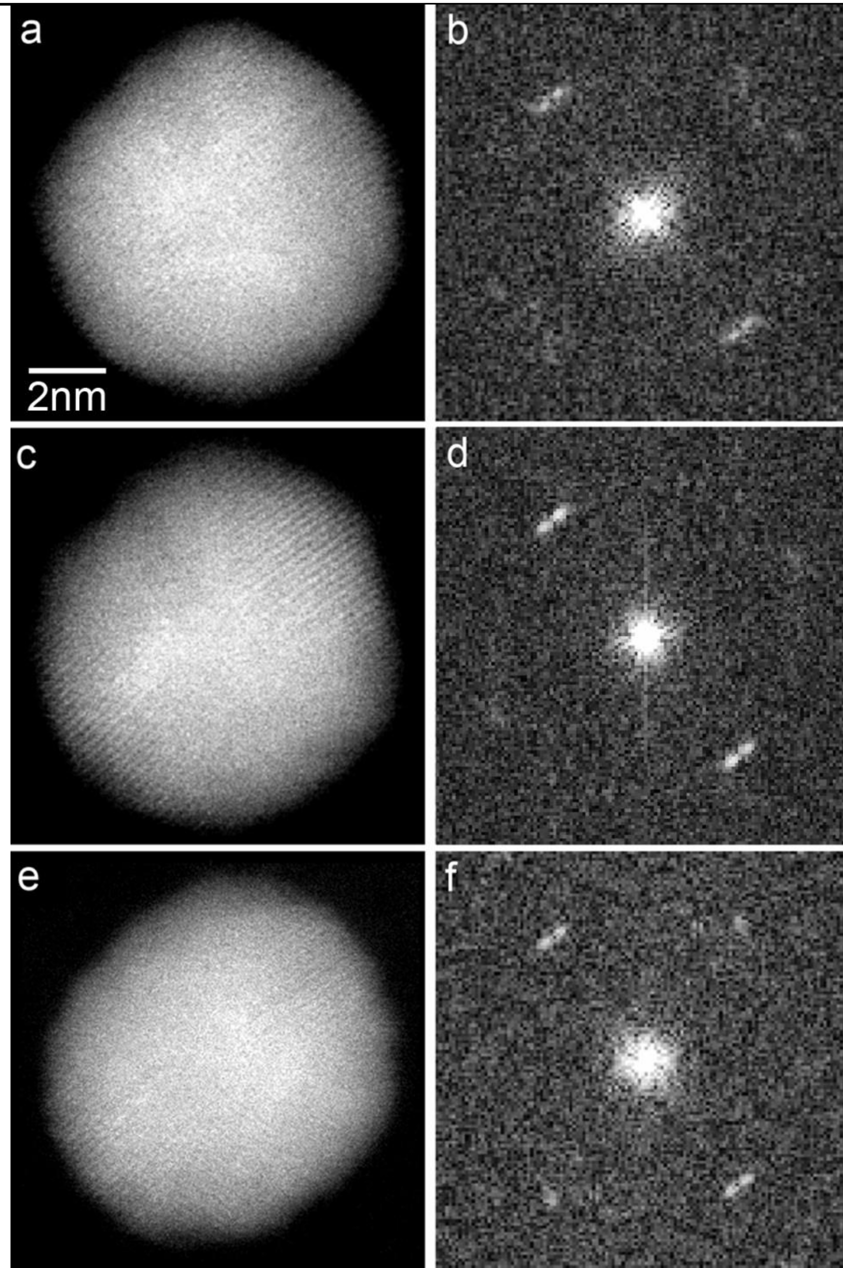

Comparison between Measured and Reconstructed Projections at 7.1°

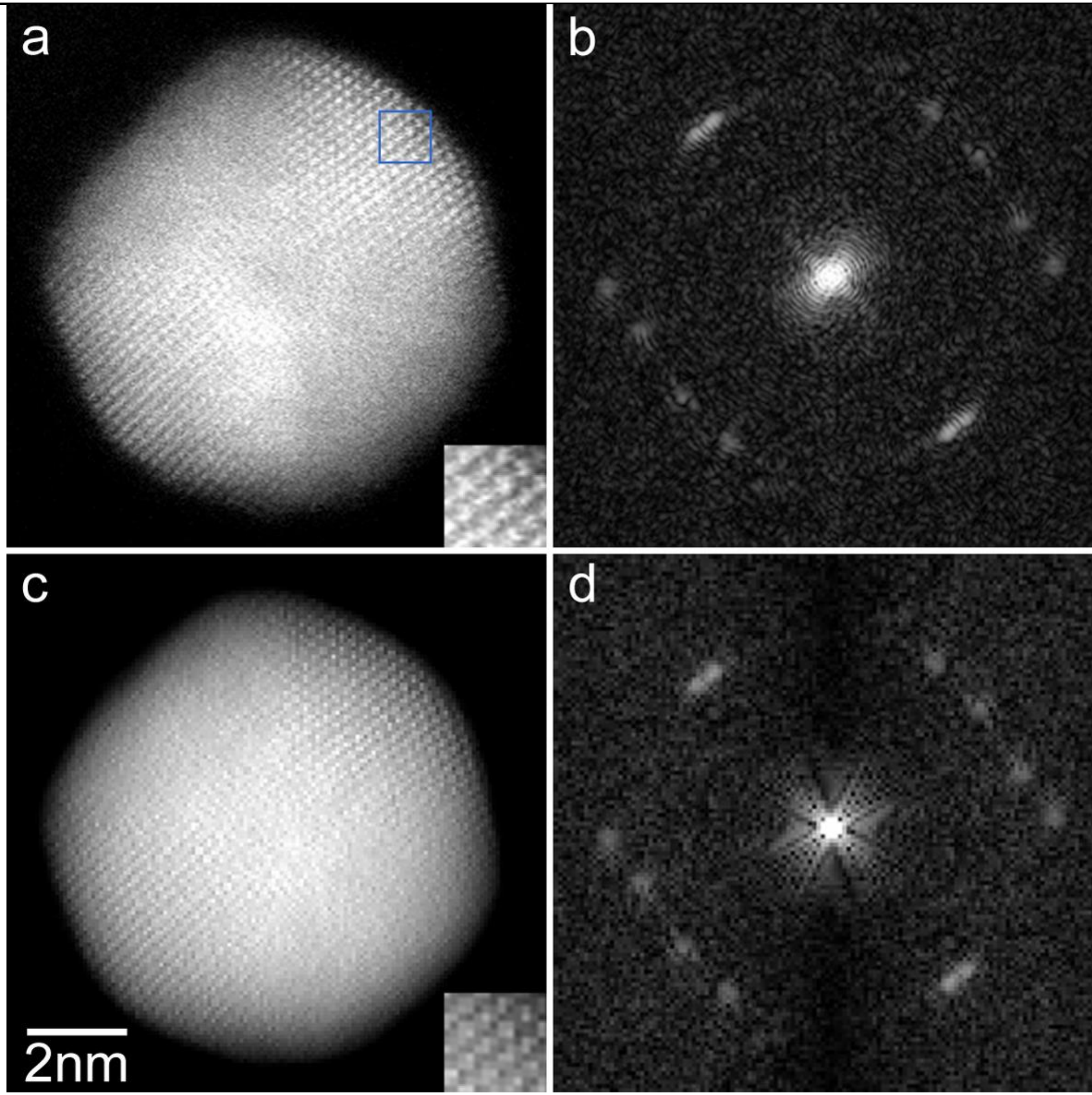

Achieving Electron Tomography at 2.4 Å Resolution

A 3.36 Å thick central slice in the XY plane

A 3.36 Å thick slice in the ZY plane

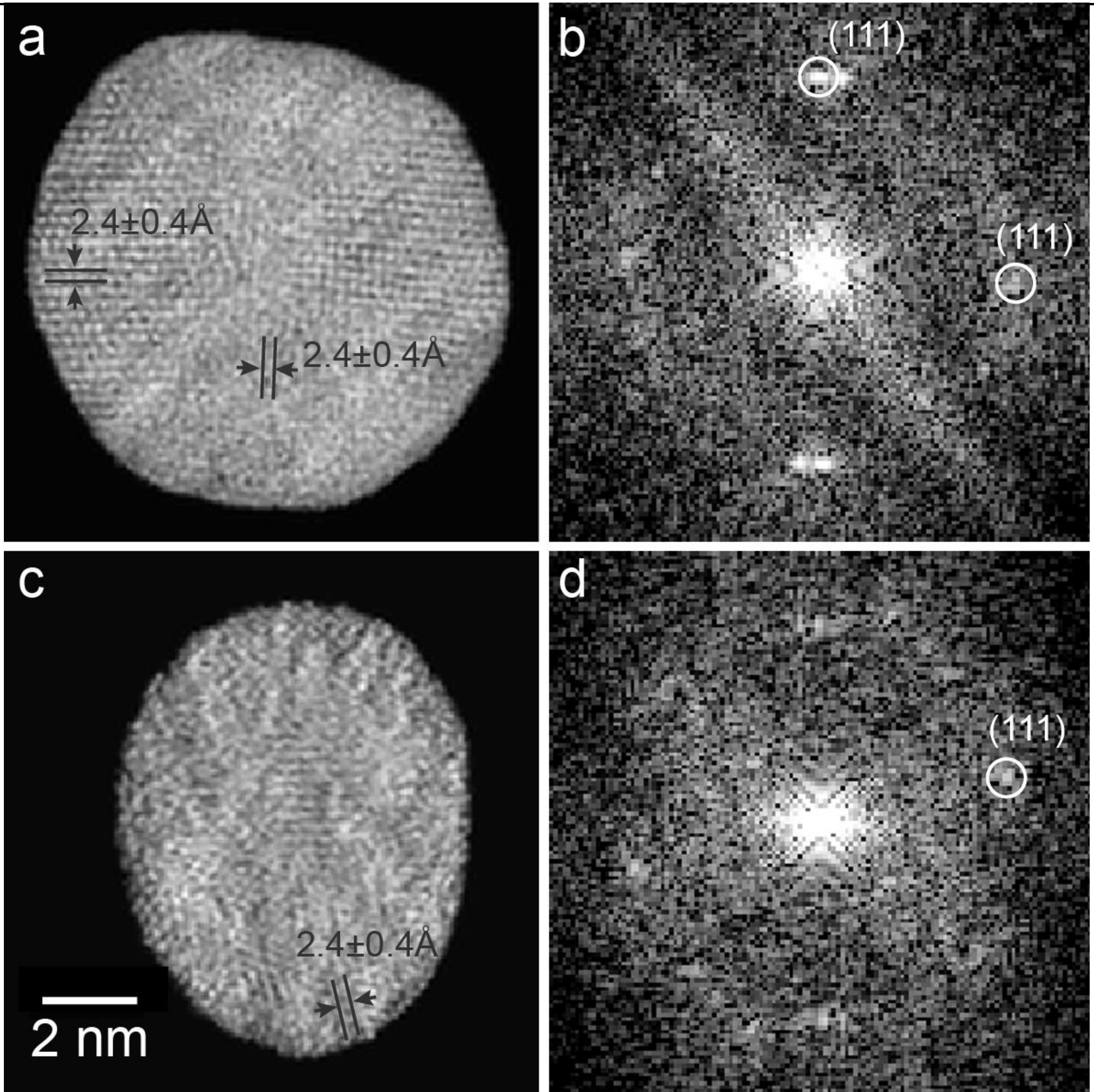

3D Volume and Surface Renderings of the Reconstructed Au Nanoparticle

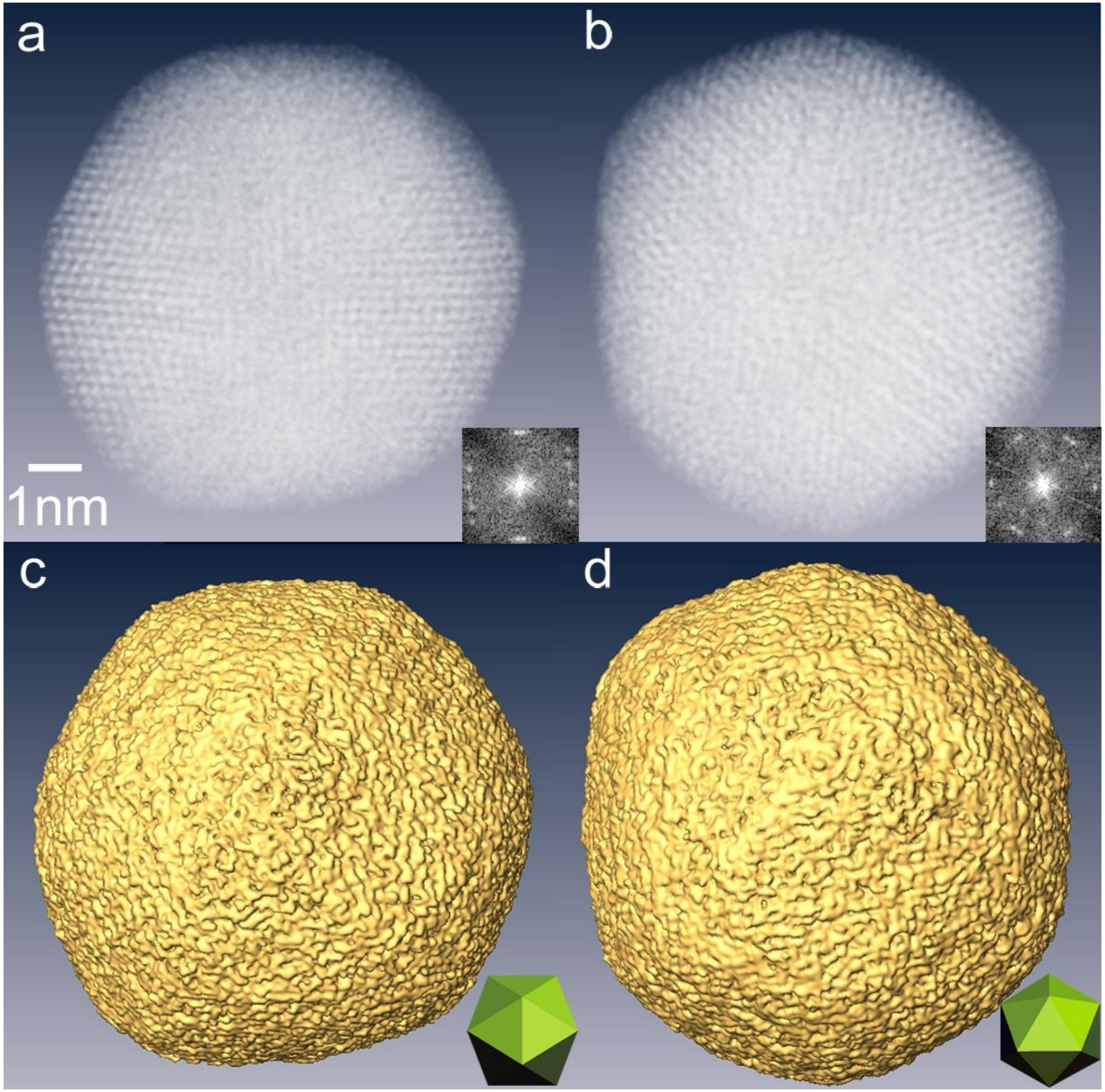

Identification of Major 3D Grains inside the Au Nanoparticle at Atomic Scale Resolution

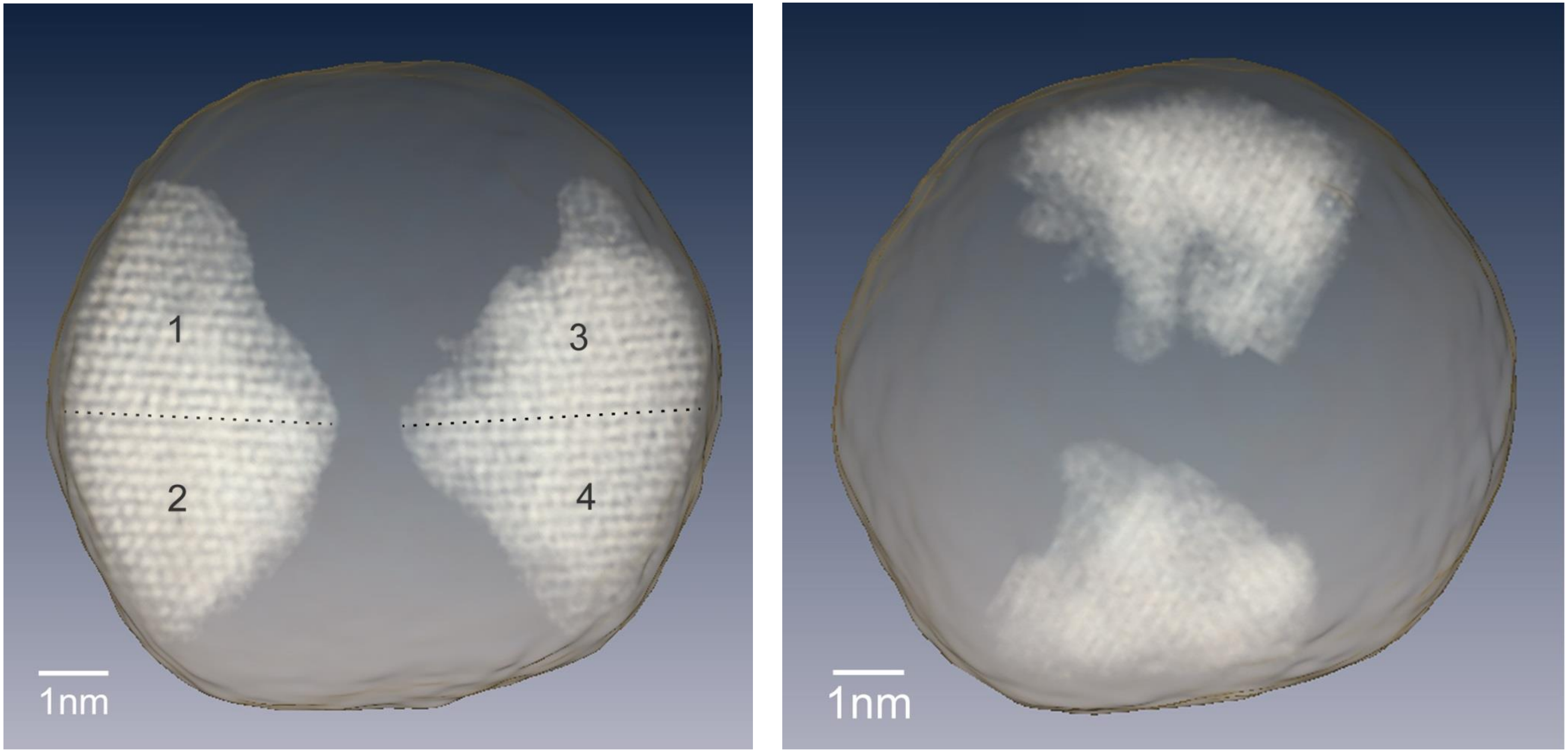

Scott, Chen, Mecklenburg, Zhu, Xu, Ercius, Dahmen, Regan, Miao, *Nature* **483**, 444-447 (2012).

Experimental STEM Tilt Series of 104 Projections Acquired from a Multiply-Twinned Pt Particle

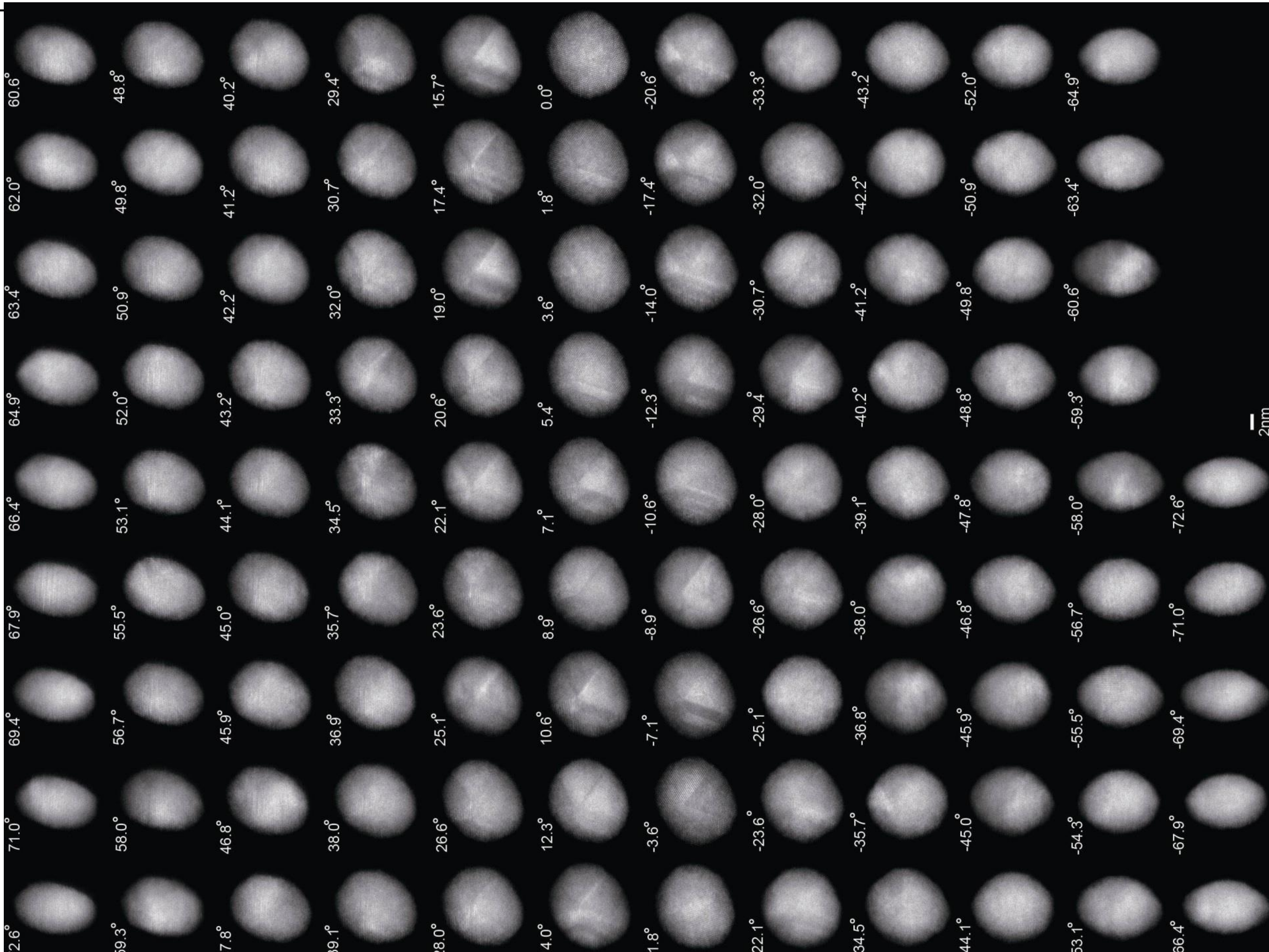

3D Reconstruction of the Pt Nanoparticle before and after Applying a 3D Fourier Filter

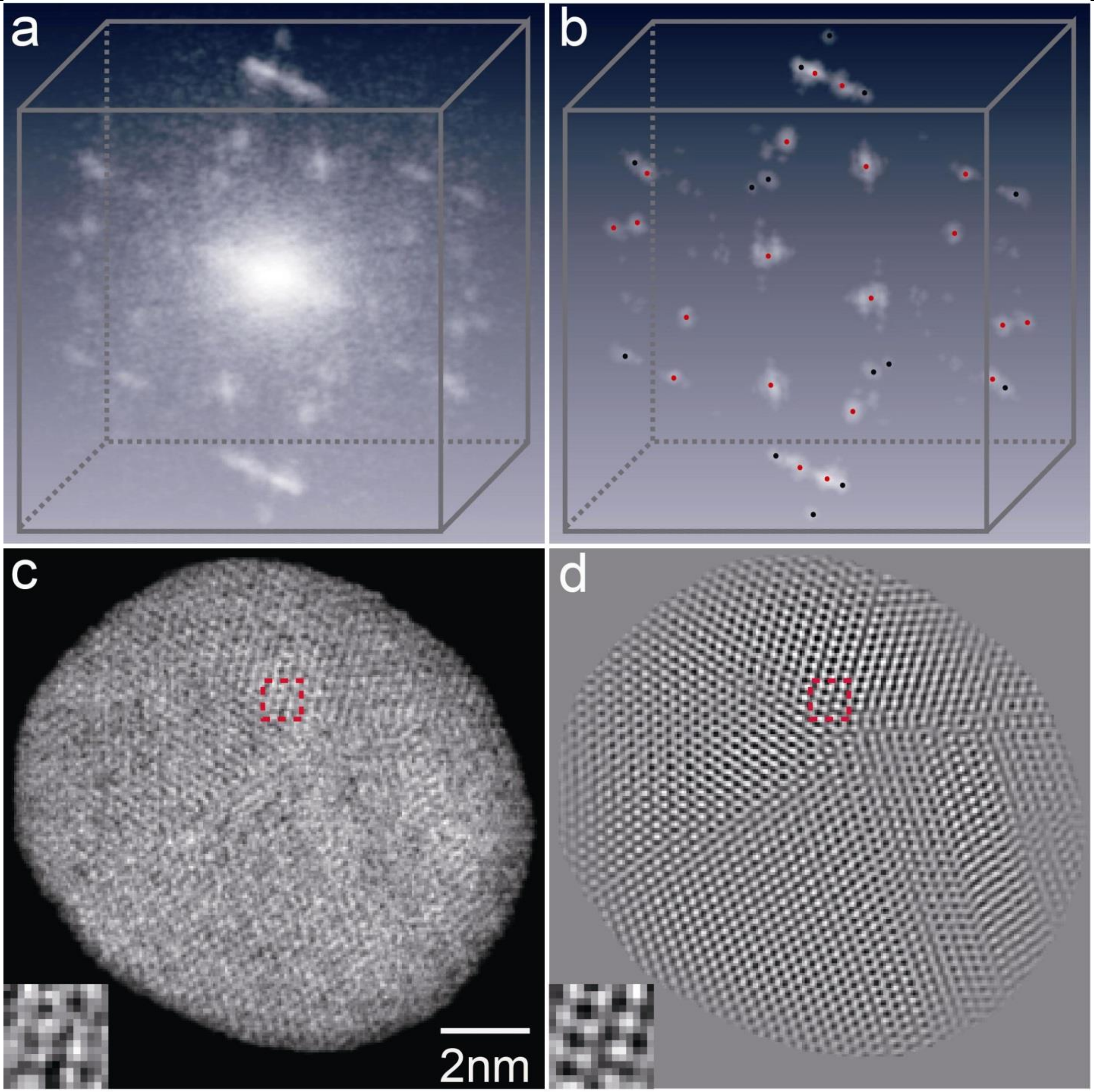

A 2.6 Å thick central slice in the XY plane

Comparison between 3D Fourier and 3D Wiener Filtering

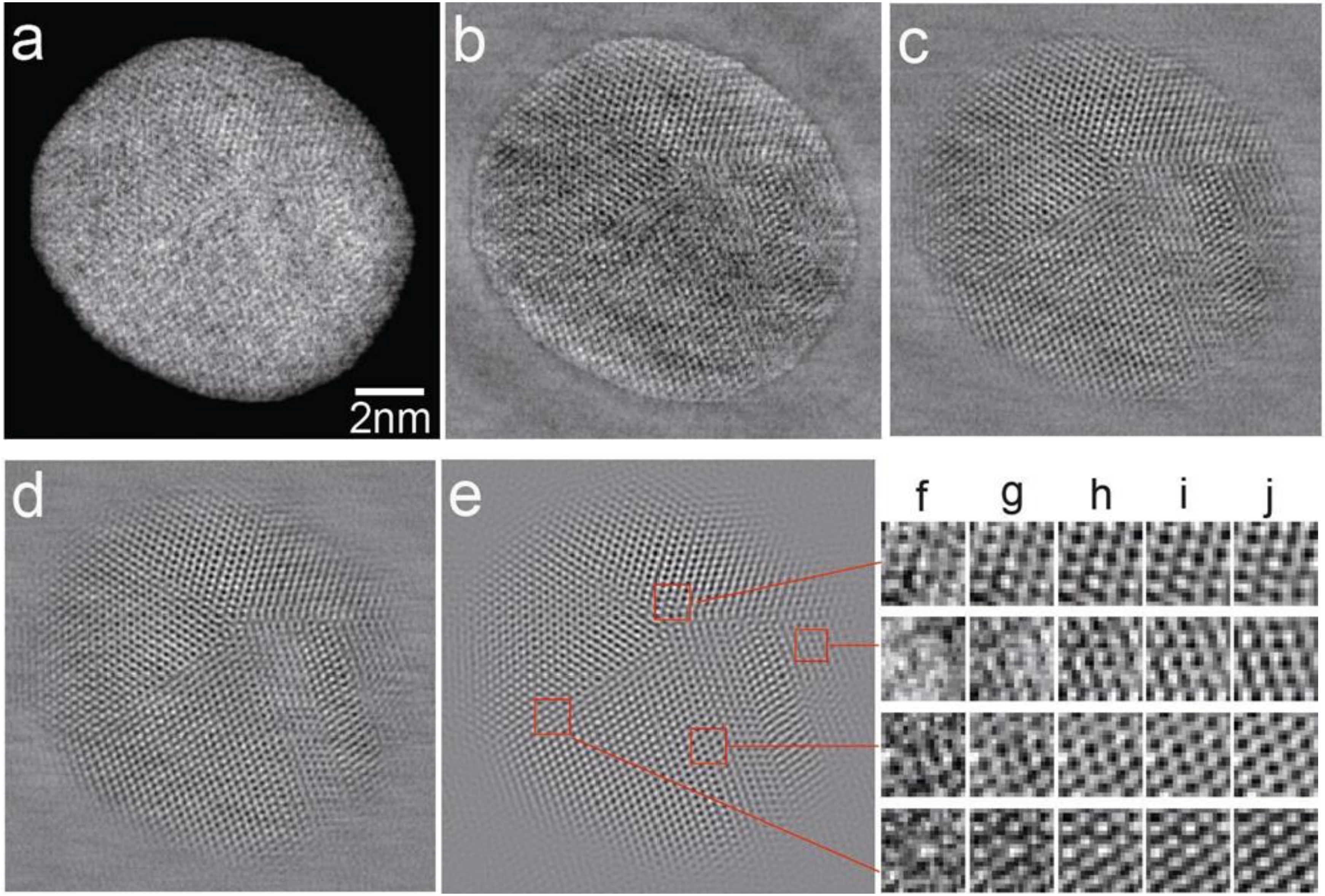

Grain Boundary Comparison between Experimental and Reconstructed Projections

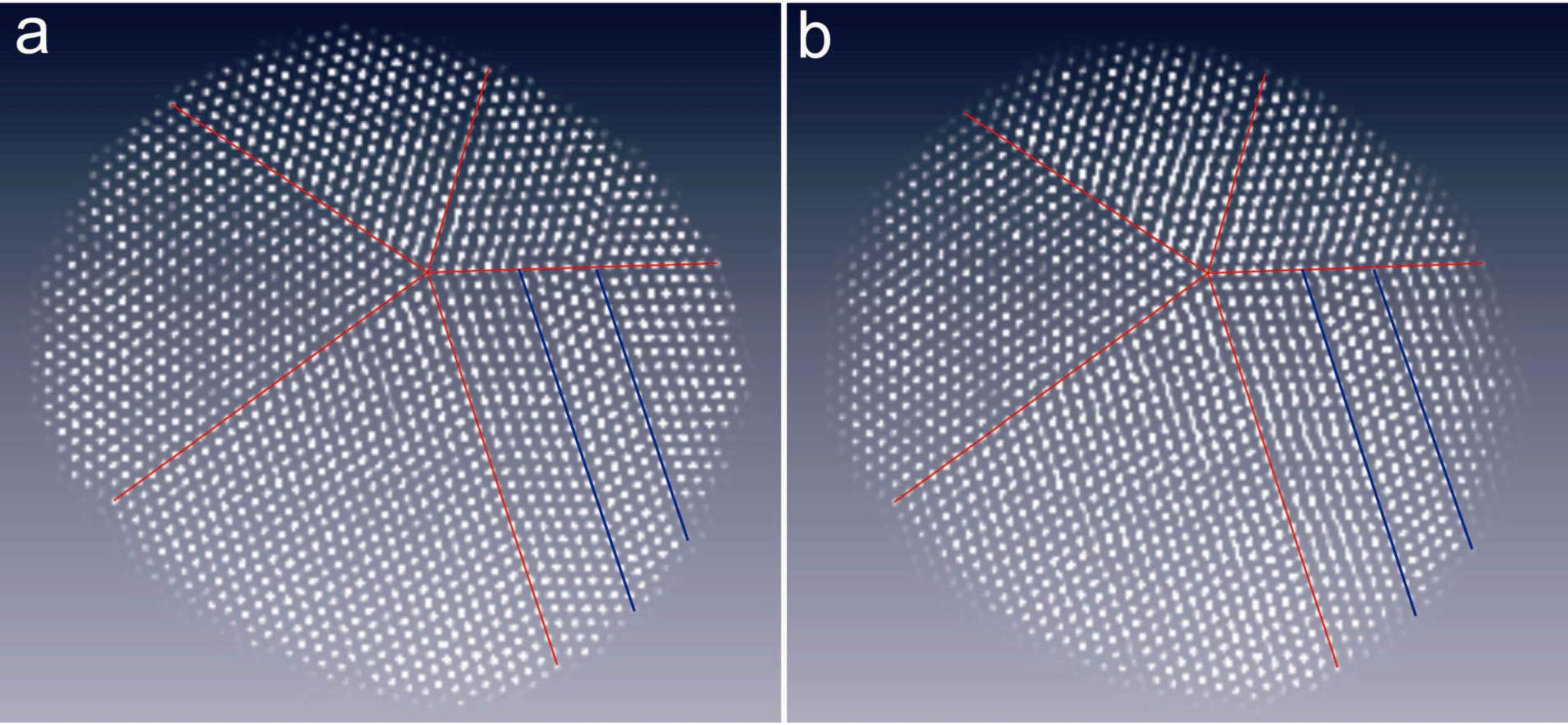

Reveal Atomic Steps at the 3D Grain Boundaries in the Pt Nanoparticle

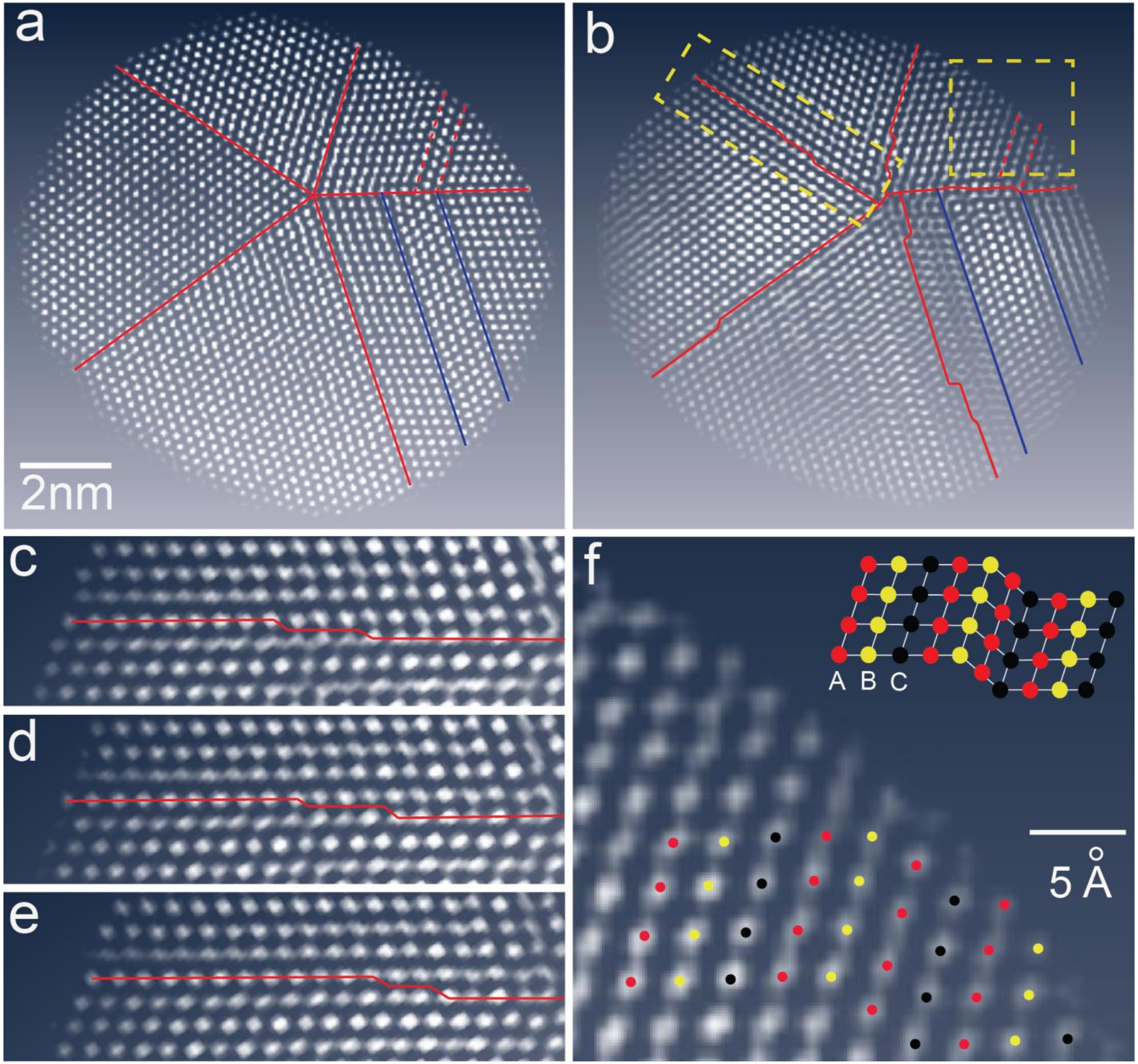

Comparison between 3D Fourier and 3D Wiener Filtering on Atomic Steps across a Twin Boundary

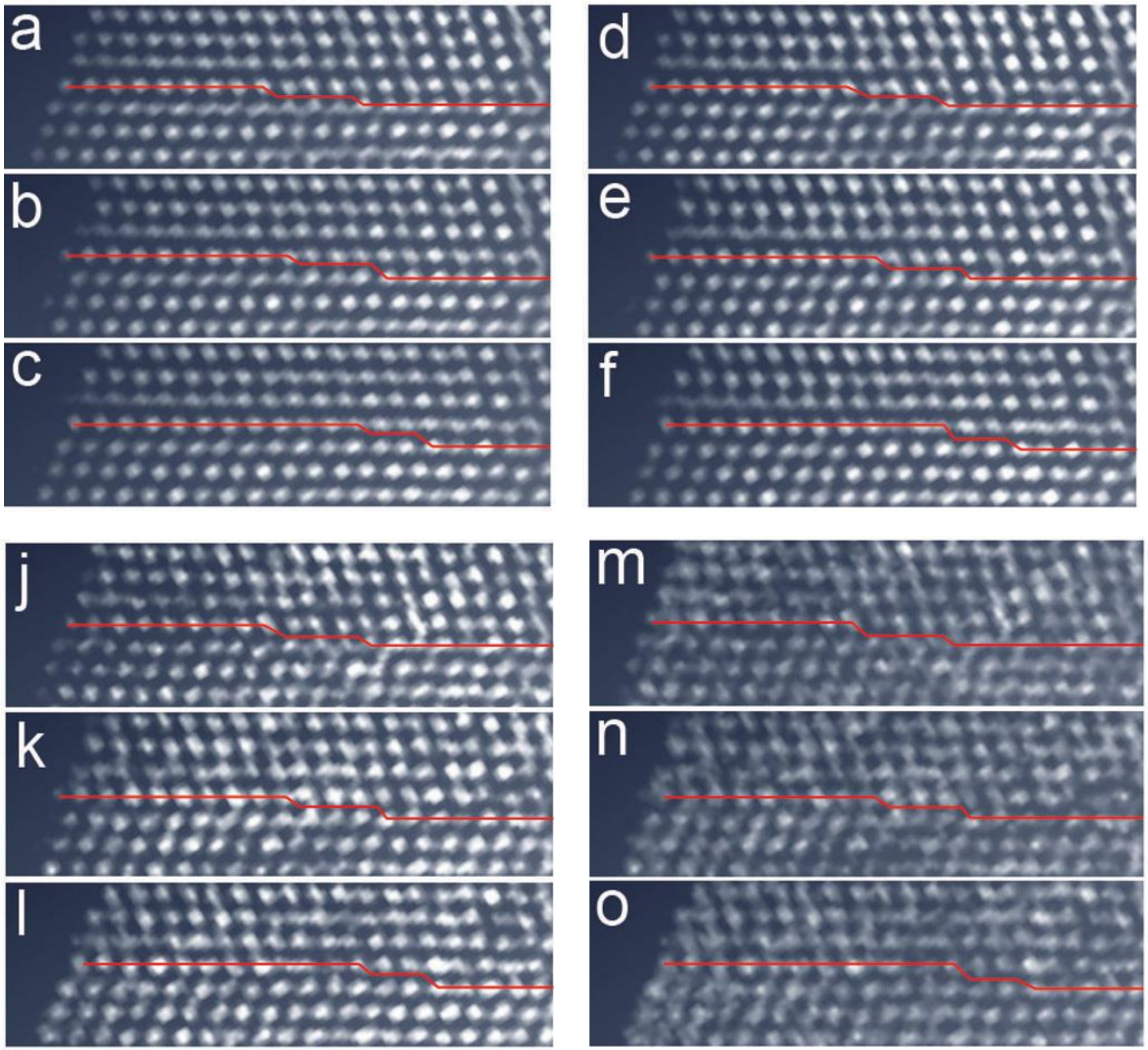

3D Fourier filtering with a threshold of 10% (a-c) and 7% (d-f).

3D Wiener filtering with $\lambda = 3$ (g-i), $\lambda = 2$ (j-l) and $\lambda = 1$ (m-o).

3D Imaging of the Core Structure of an Edge Dislocation at Atomic Resolution

A 7.9 Å thick internal slice

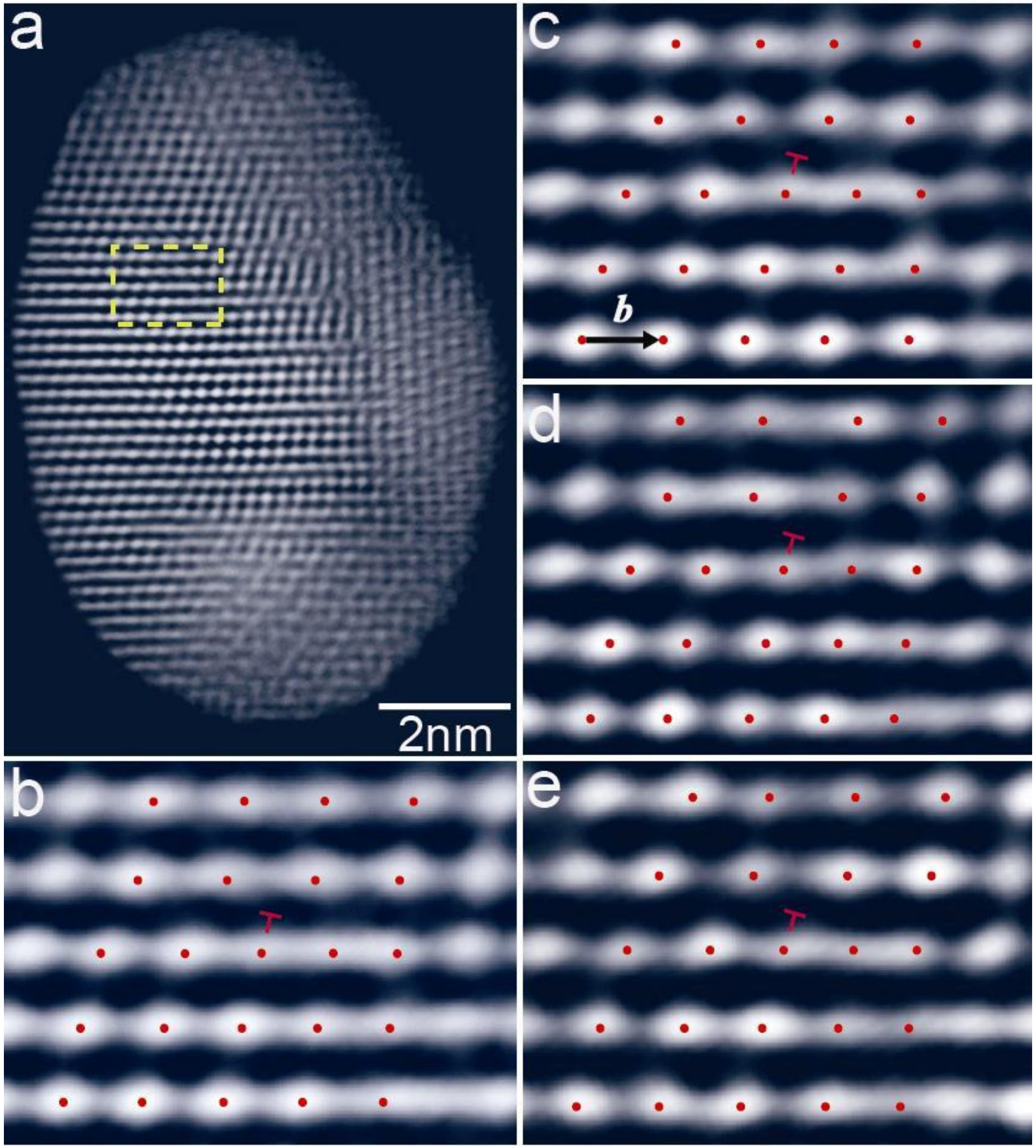

Three 2.6 Å atomic layers sectioning through the slice of (b)

$$\boldsymbol{b} = \frac{1}{2}[101]$$

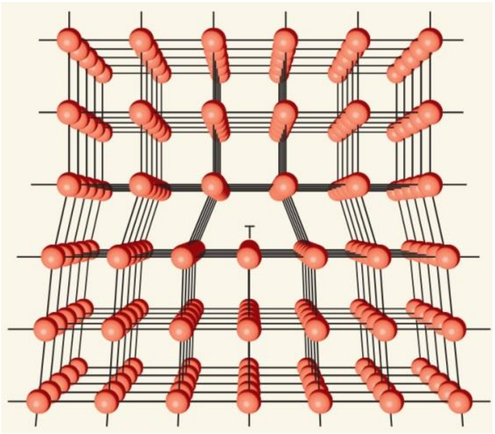

Edge dislocation in a simple cubic lattice

3D Imaging of a Screw Dislocation at Atomic Resolution
(A 5.3 Å Thick Internal Slice)

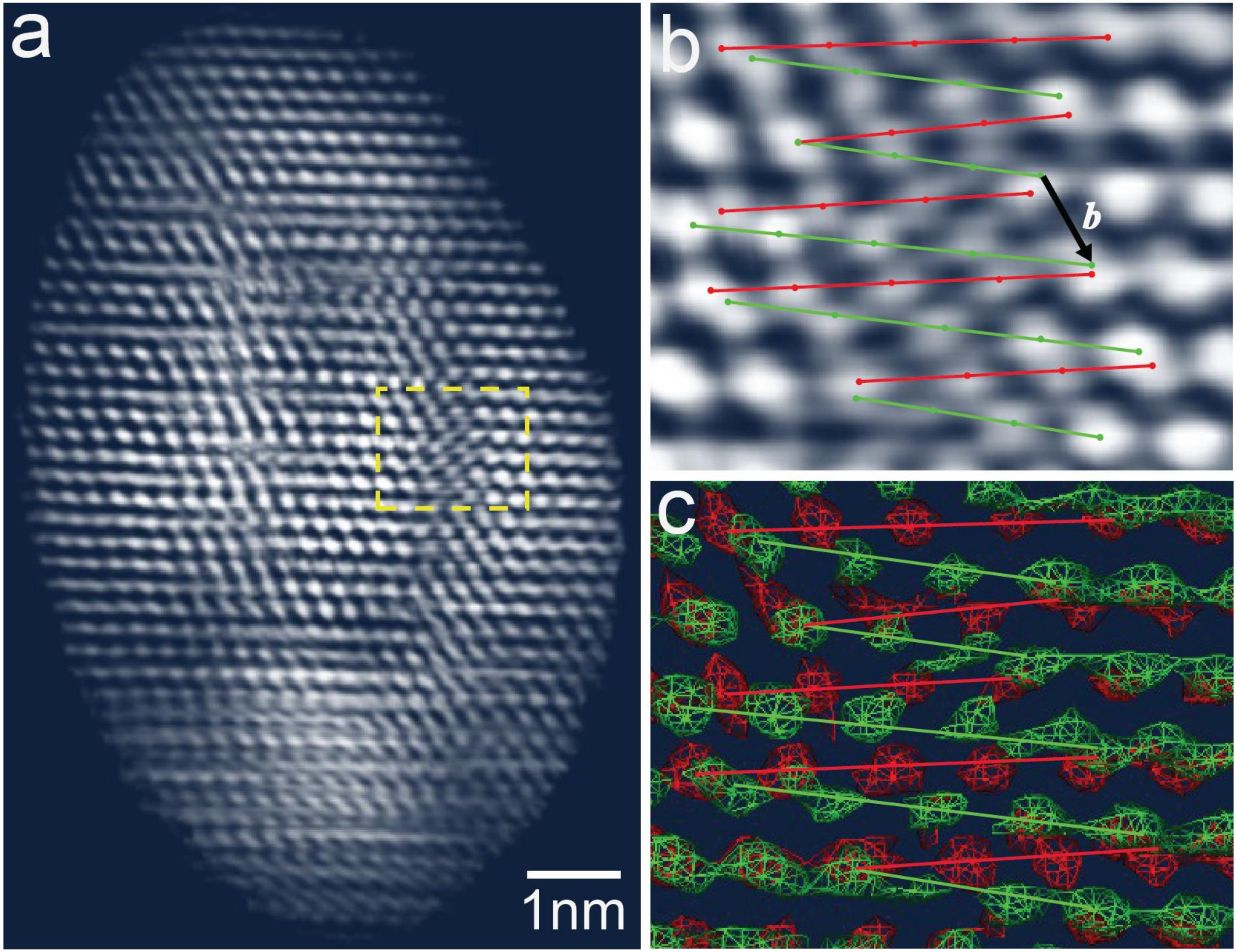

$$\boldsymbol{b} = \frac{1}{2}\left[01\,\bar{1}\right]$$

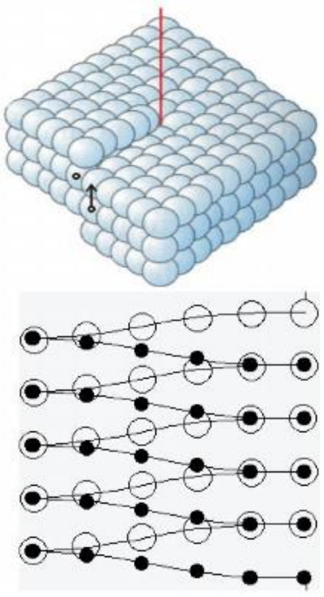

Chen, Zhu, White, Chiu, Scott, Regan, Marks, Huang & Miao, *Nature* **496**, 74-77 (2013).

3D Fourier filtering codes and data sets: www.physics.ucla.edu/research/imaging/dislocations

Association of the Screw Dislocation with Atomic Steps at a Twin Boundary

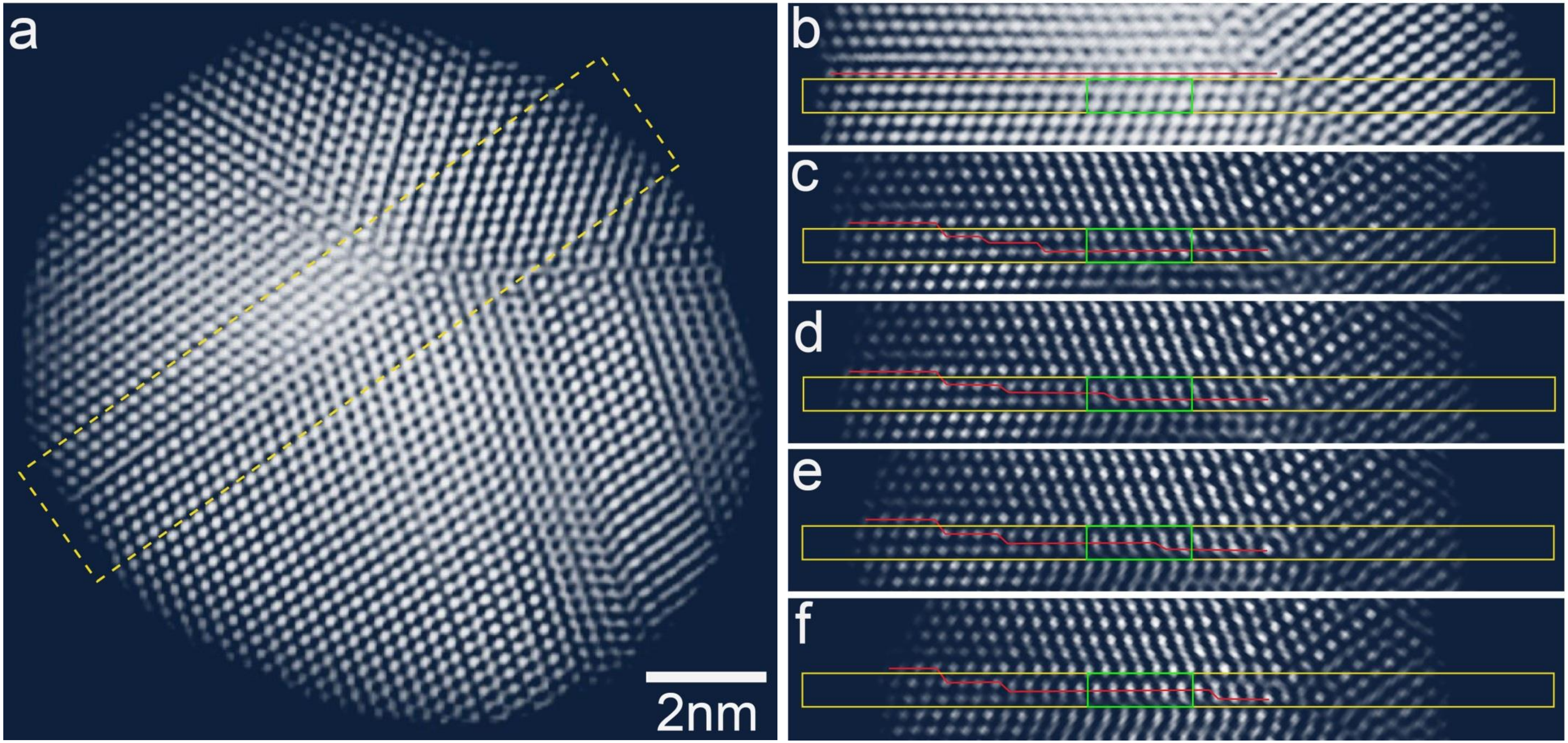

The dislocations and the atomic steps at the twin boundaries appear to be stress-relief mechanism.

Observation of Nearly All the Atoms in the Pt Nanoparticle

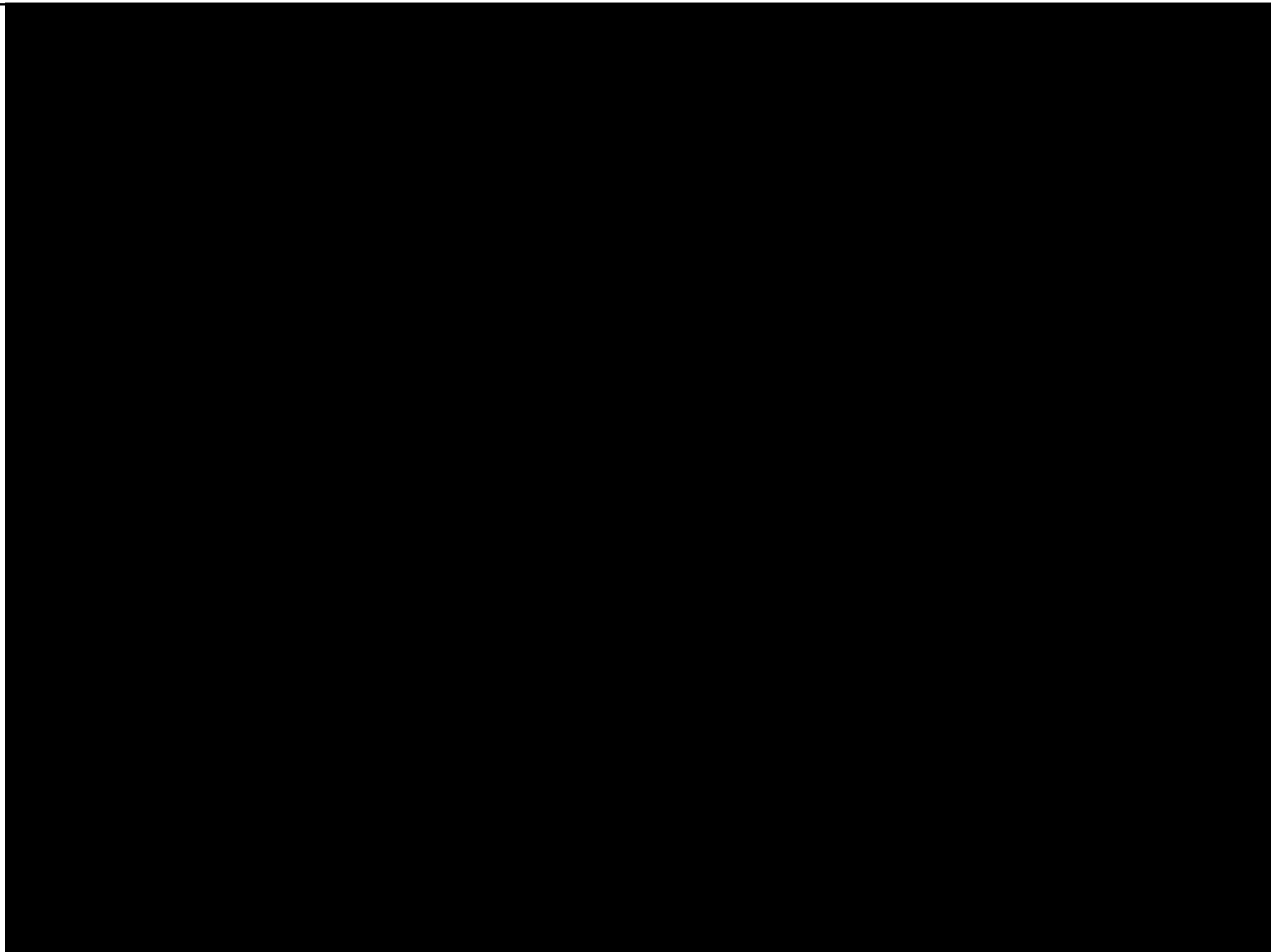

www.nature.com/nature/videoarchive/nano-imaging
(Nature video with > 780,000 YouTube views)

Determining the Coordinates of Individual Atoms with a 3D Precision of ~19 pm

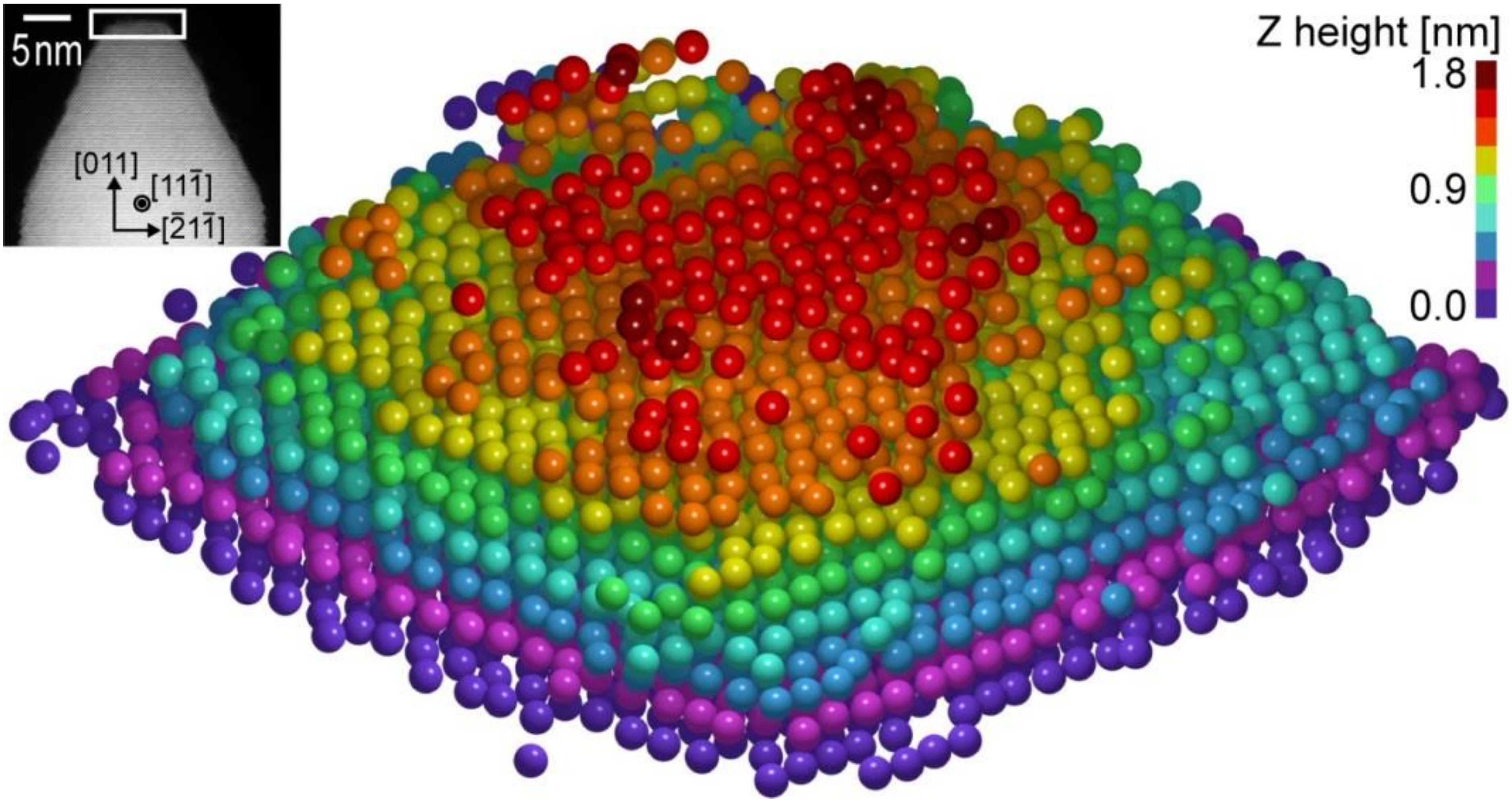

Tip of a tungsten needle, shown from layers 1 (dark red) to 9 (purple)
(Number of atoms: 3,769)

3D Identification of a Point Defect and Atomic Displacements

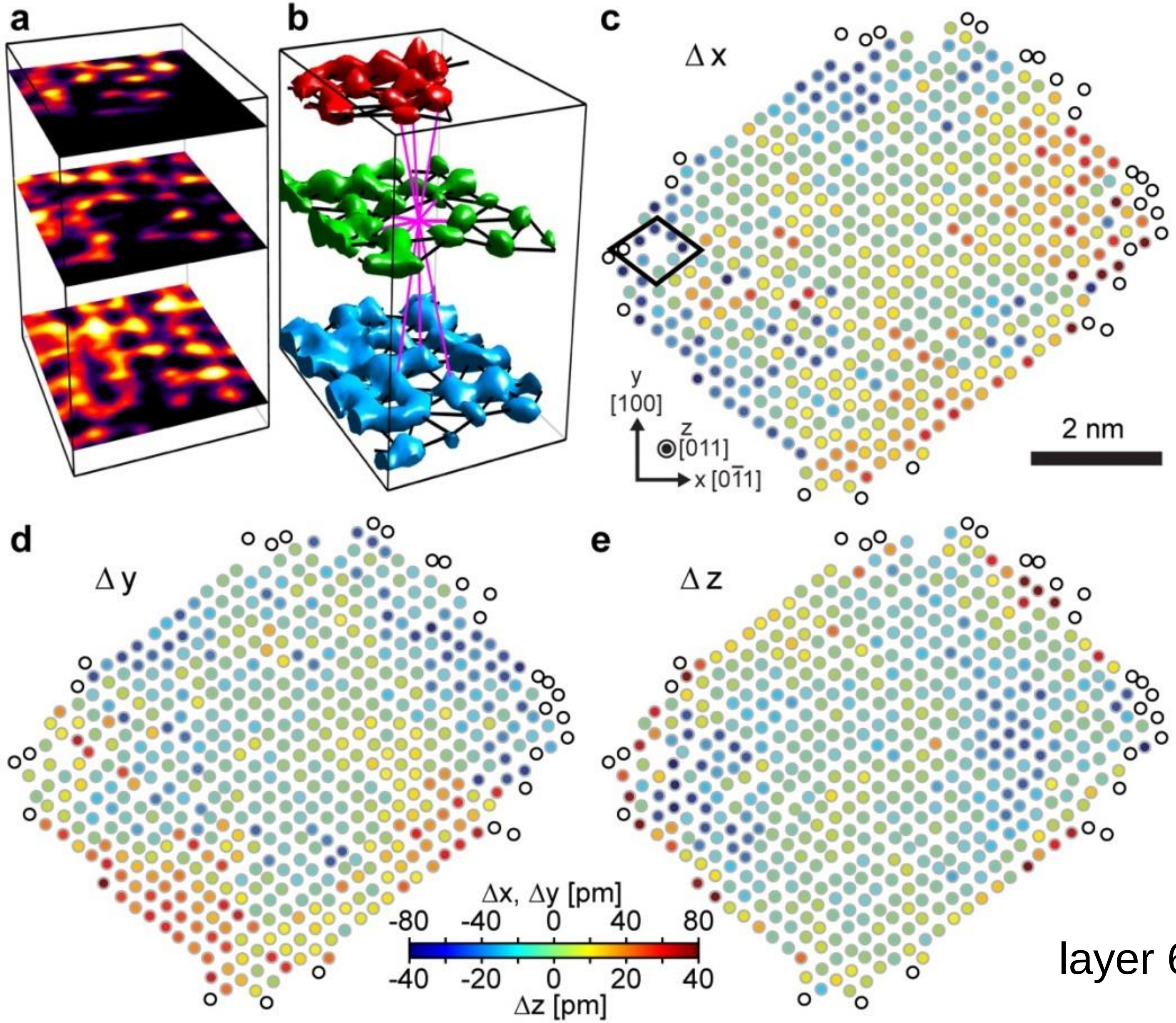

layer 6

3D Measurements of the Atomic Displacement Field and Full Strain Tensor

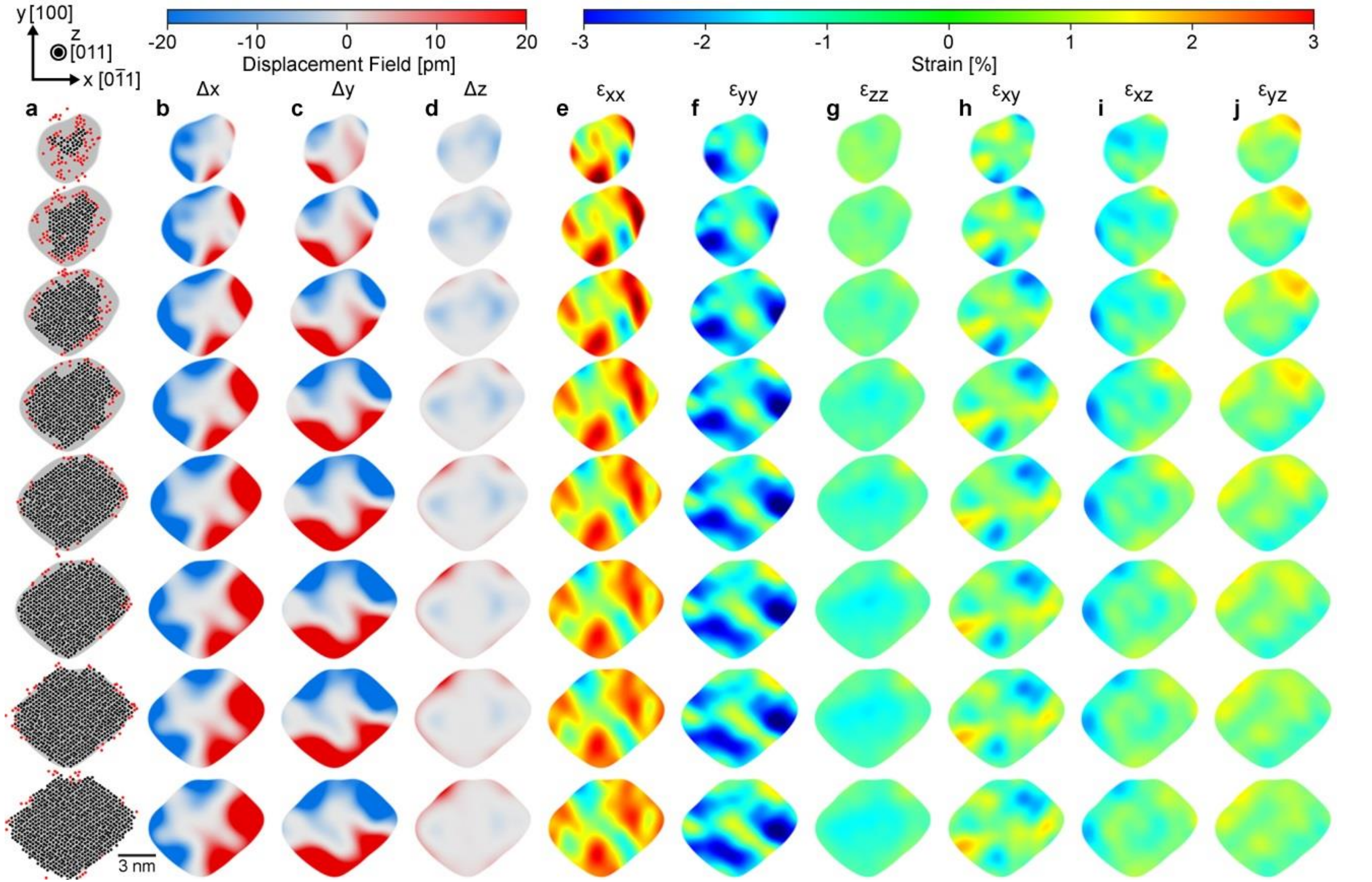

Xu, Chen, Wu, Scott, Theis, Ophus, Bartels, Yang, Ramezani-Dakhel, Sawaya, Heinz, Marks, Ercius, Miao, under review.

Origin of the Strain Field

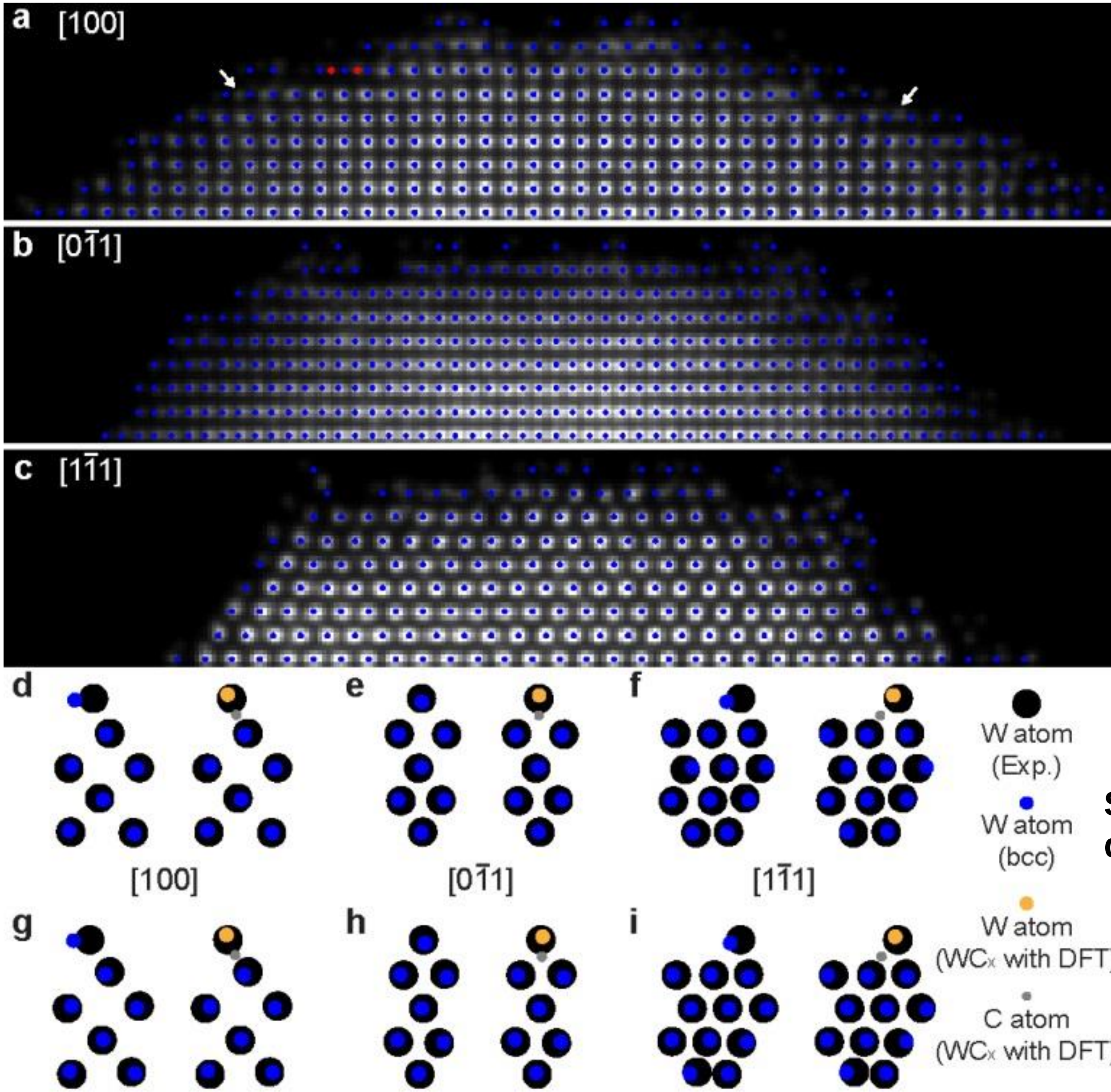

Surface WC_x and diffusion of C atoms

Verification of the Full Strain Tensor Using MD Simulations

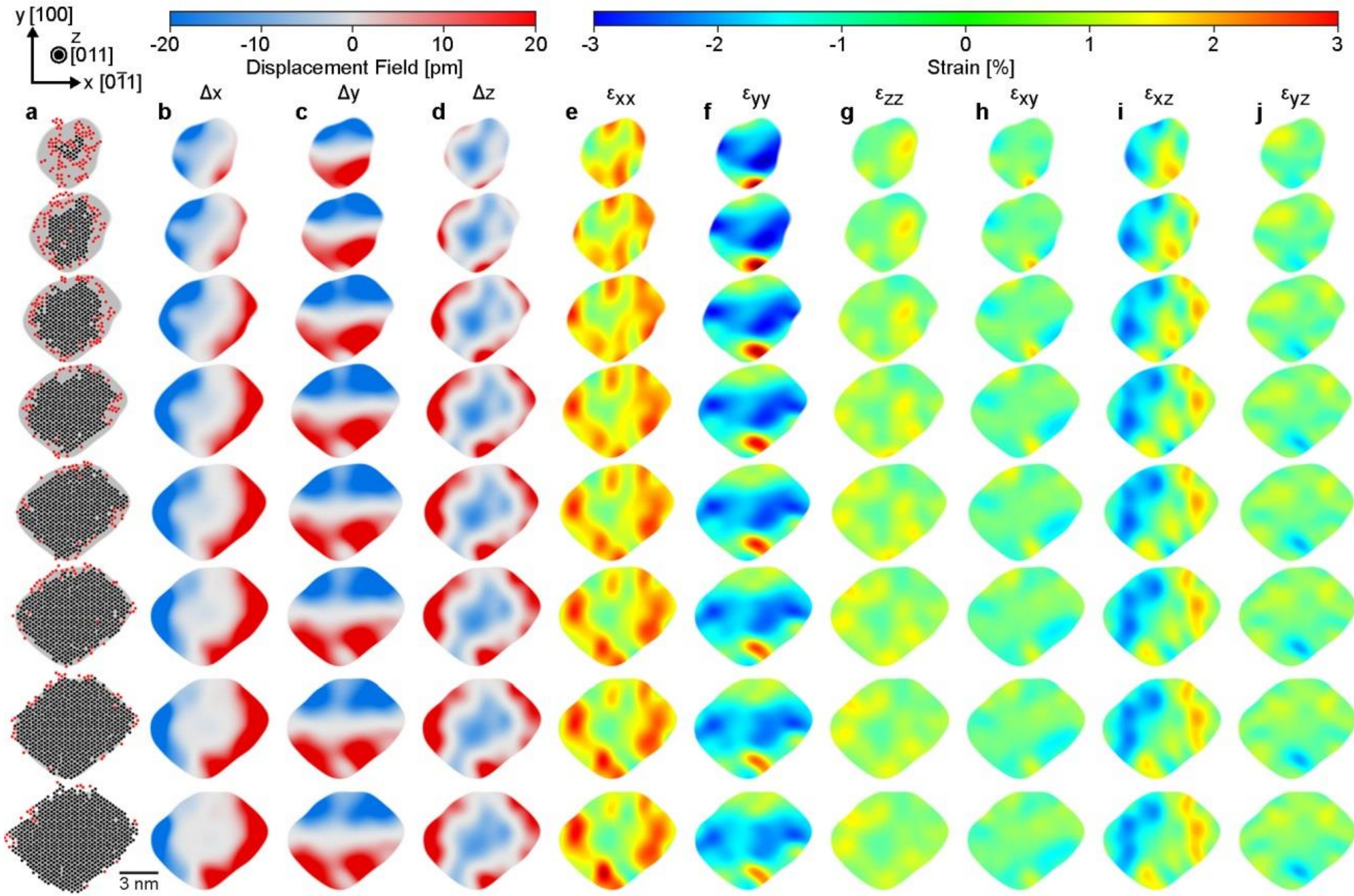

Cryo-Electron Tomography Tilt-Series of Hemocyanin Macromolecules

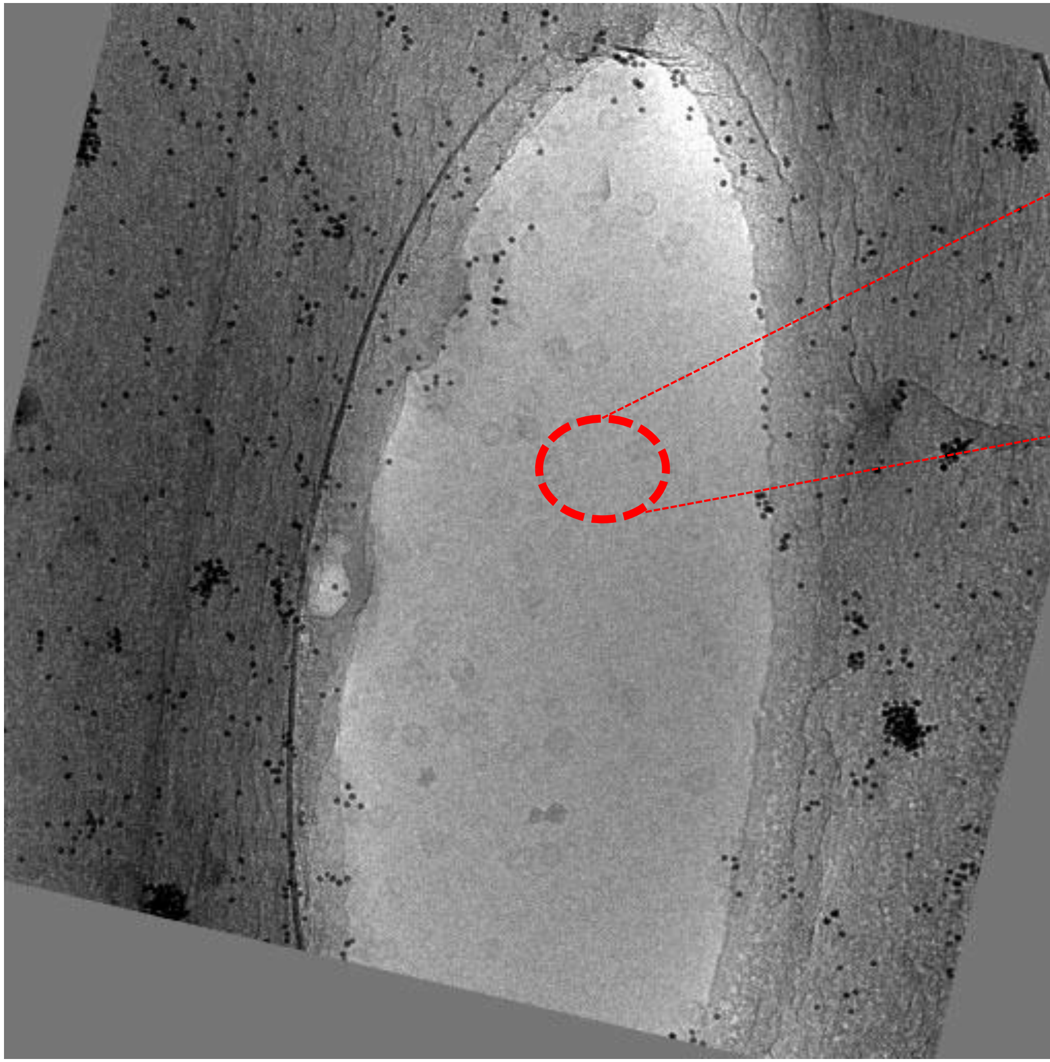

3D model averaged from many identical copies

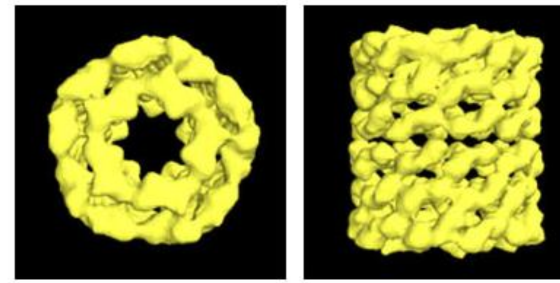

Hemocyanins carry oxygen in the blood of most molluscs, and some arthropods. Similar function as hemoglobin in human.

Comparison among EST, WBP, ART and SART Reconstructions

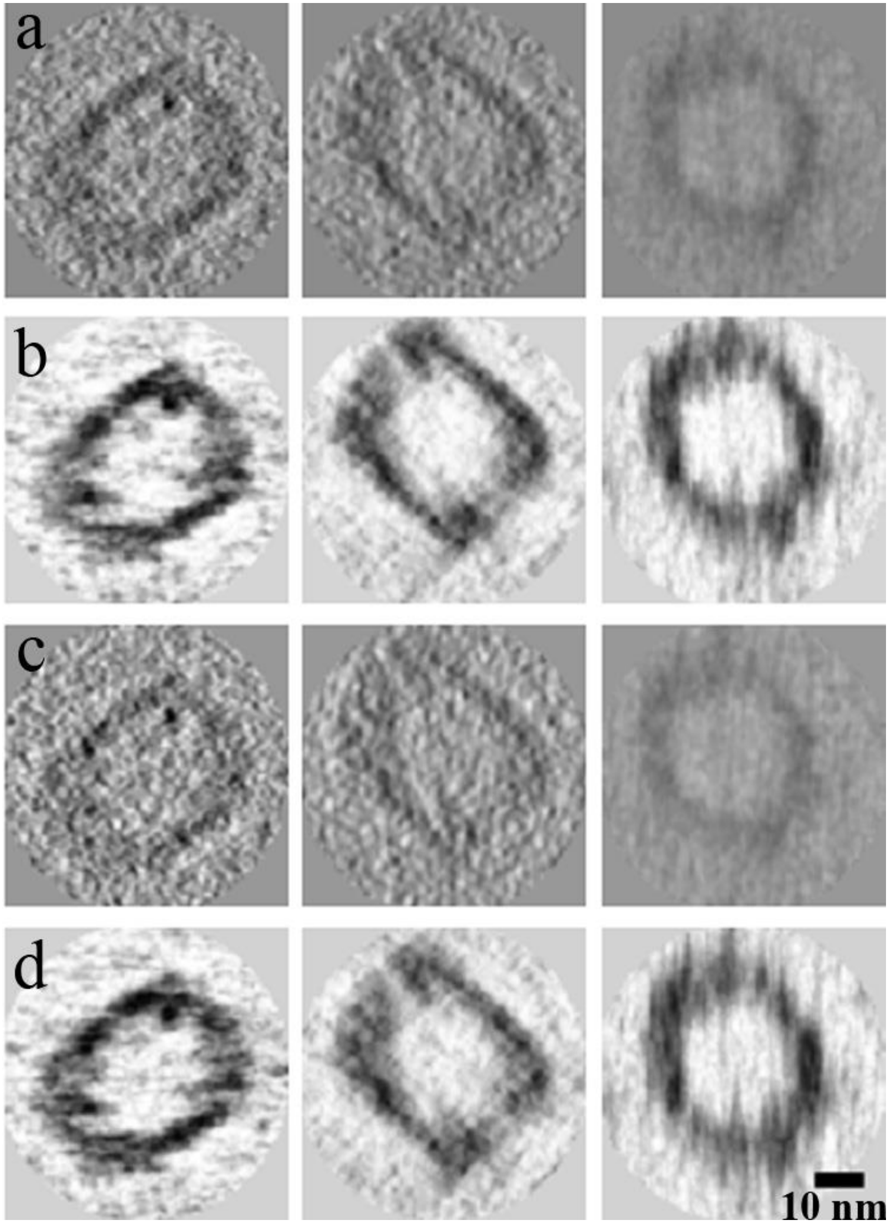

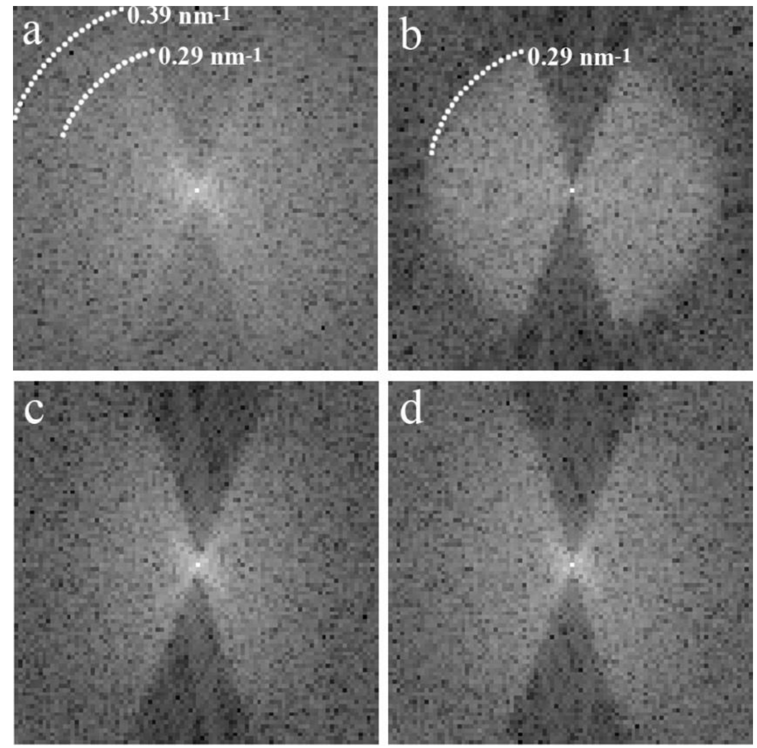

Surface Renderings of a Hemocyanin Molecule Reconstructed by WBP and EST

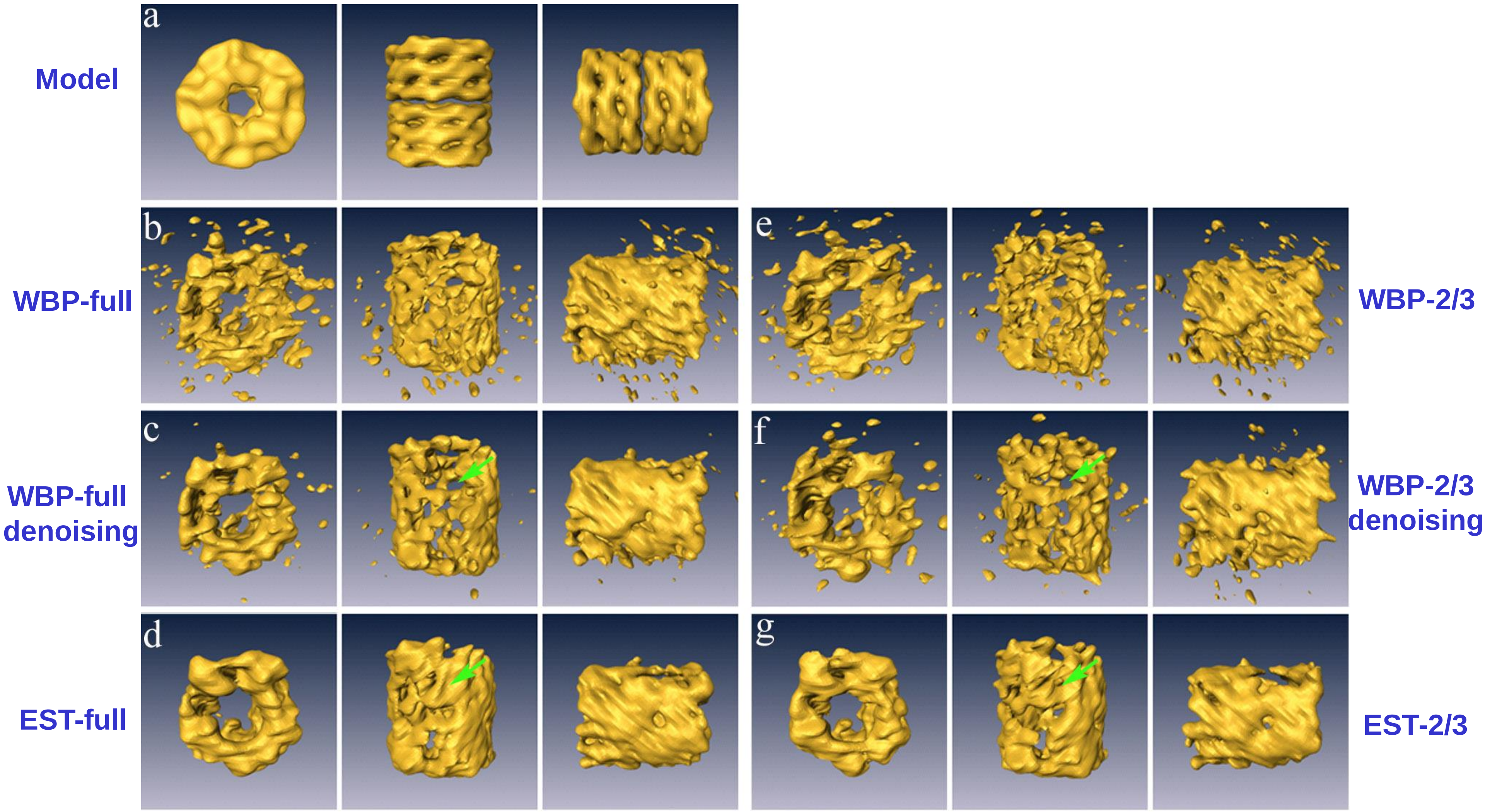

Quantitative Comparison among Different Reconstruction Methods

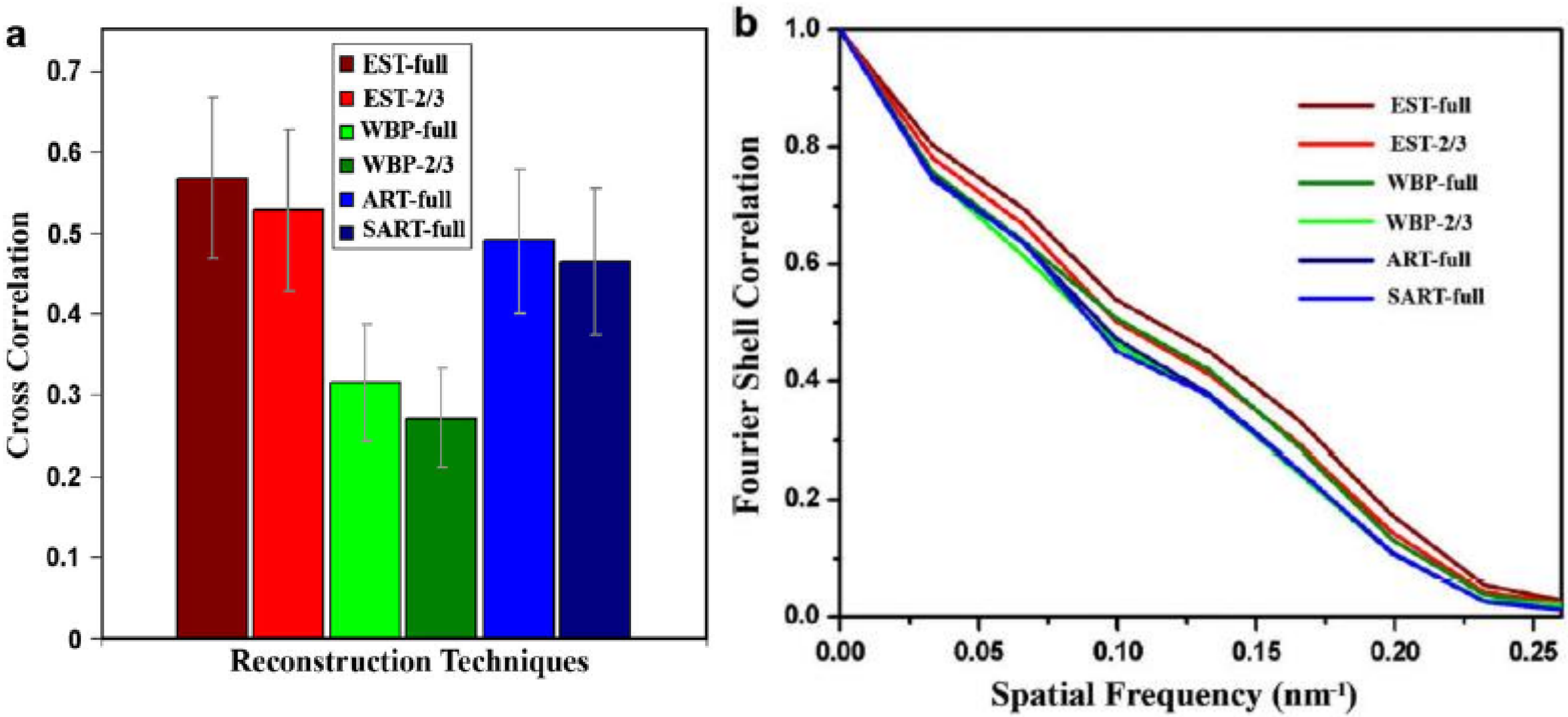

EST improves a resolution of 5 Å over WBP, 18 Å over ART, and 21 Å over SART.

Lee, Fahimian, Jensen, Miao et al., *J. Struct. Biol*. **164**, 221 (2008).

3D Reconstructions of an Intact Bacterial Cell with EST

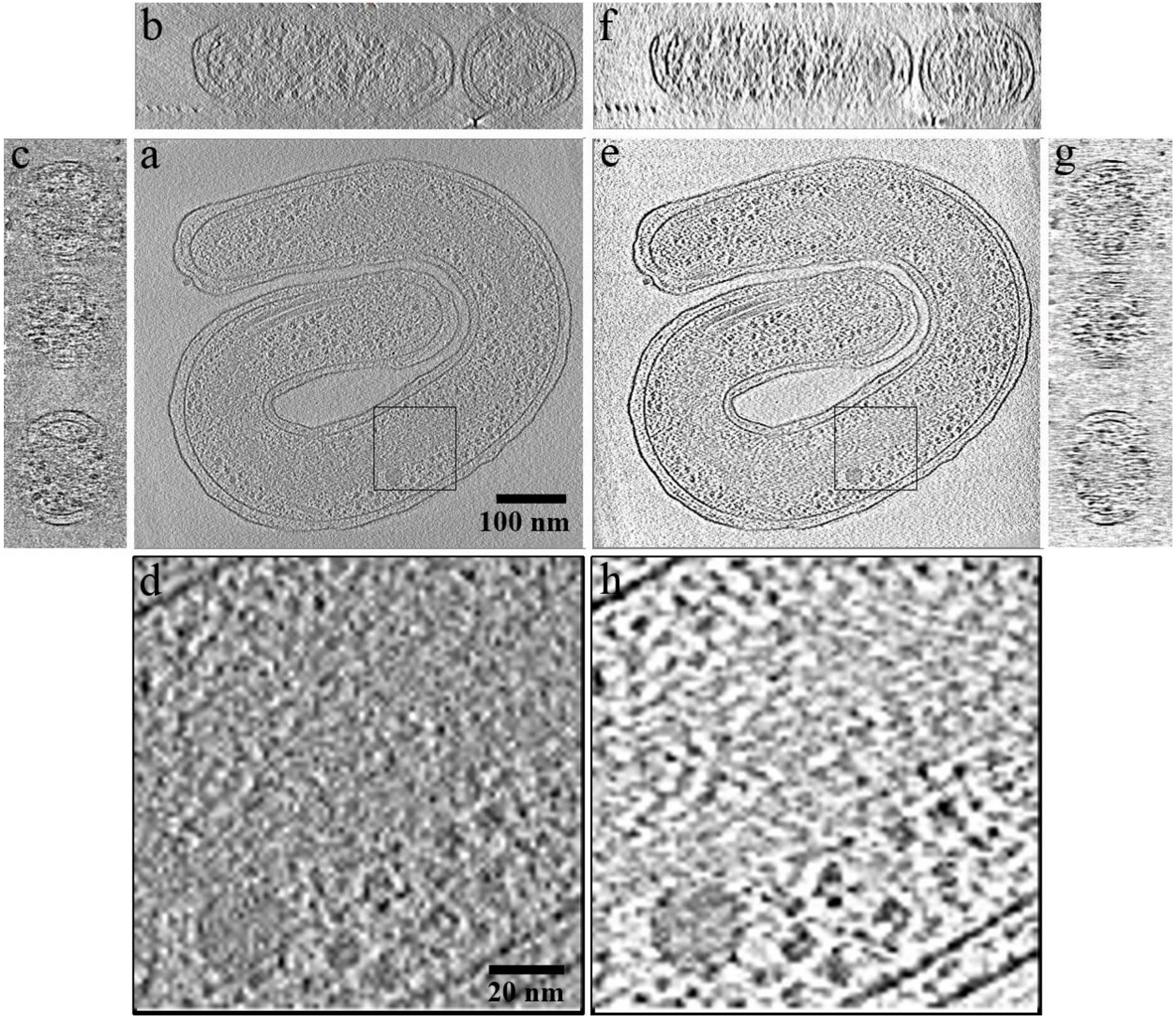

Lee, Fahimian, Jensen, Miao et al., *J. Struct. Biol*. **164**, 221 (2008).

Application of EST to X-ray Phase Contrast Imaging

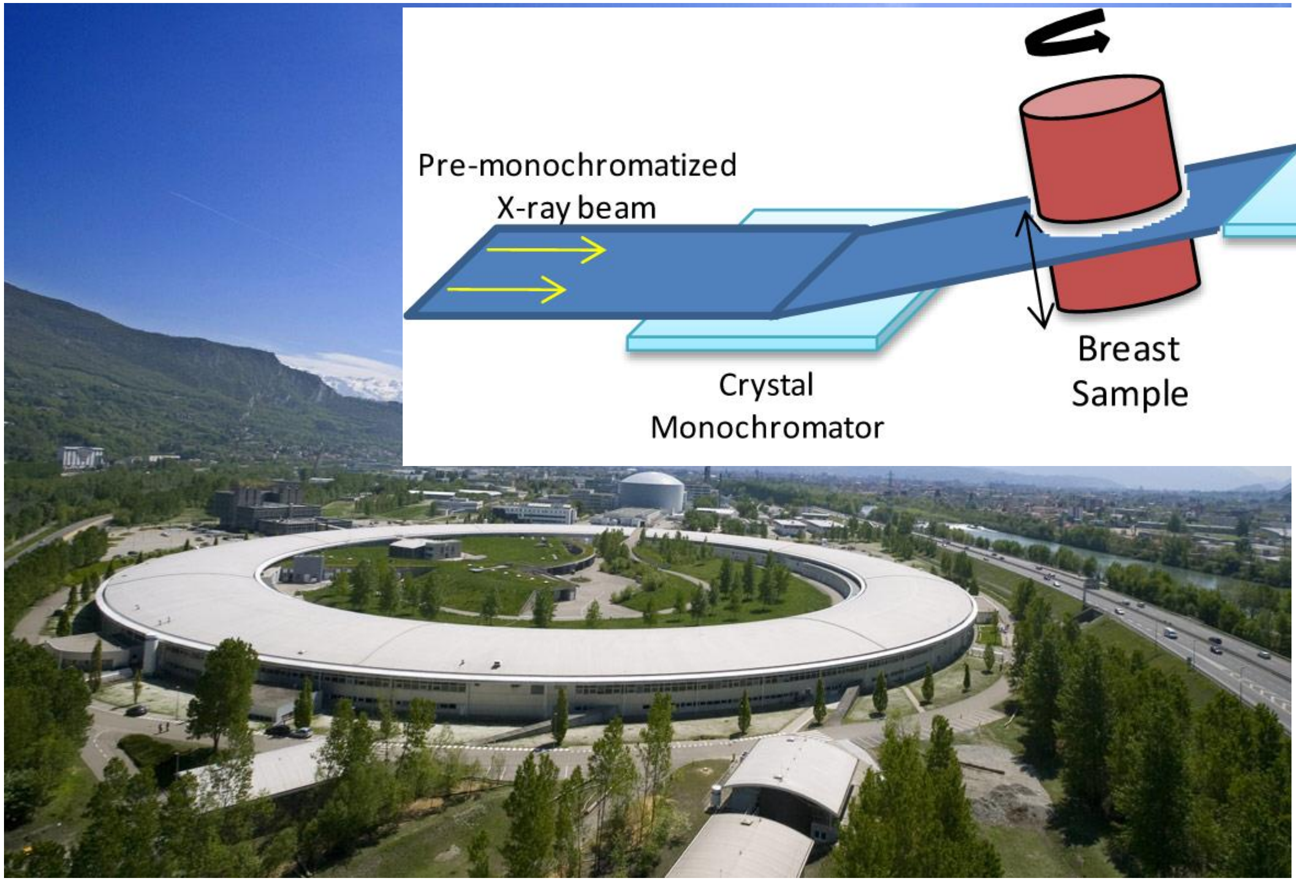

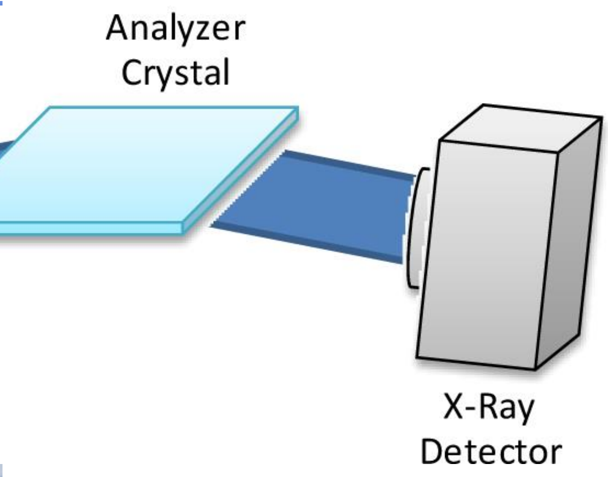

ESRF – The European Synchrotron

X-ray energy: 60 keV
Detector pixel size: 92 μm
Breast cancer sample thickness: 9 cm
Acquisition time (2,000 projs.): ~30 minutes

Bravin *et al*., *Phys. Med. Biol*. **52**, 2197–2211 (2007).

Comparison Between FBP and EST Reconstructions

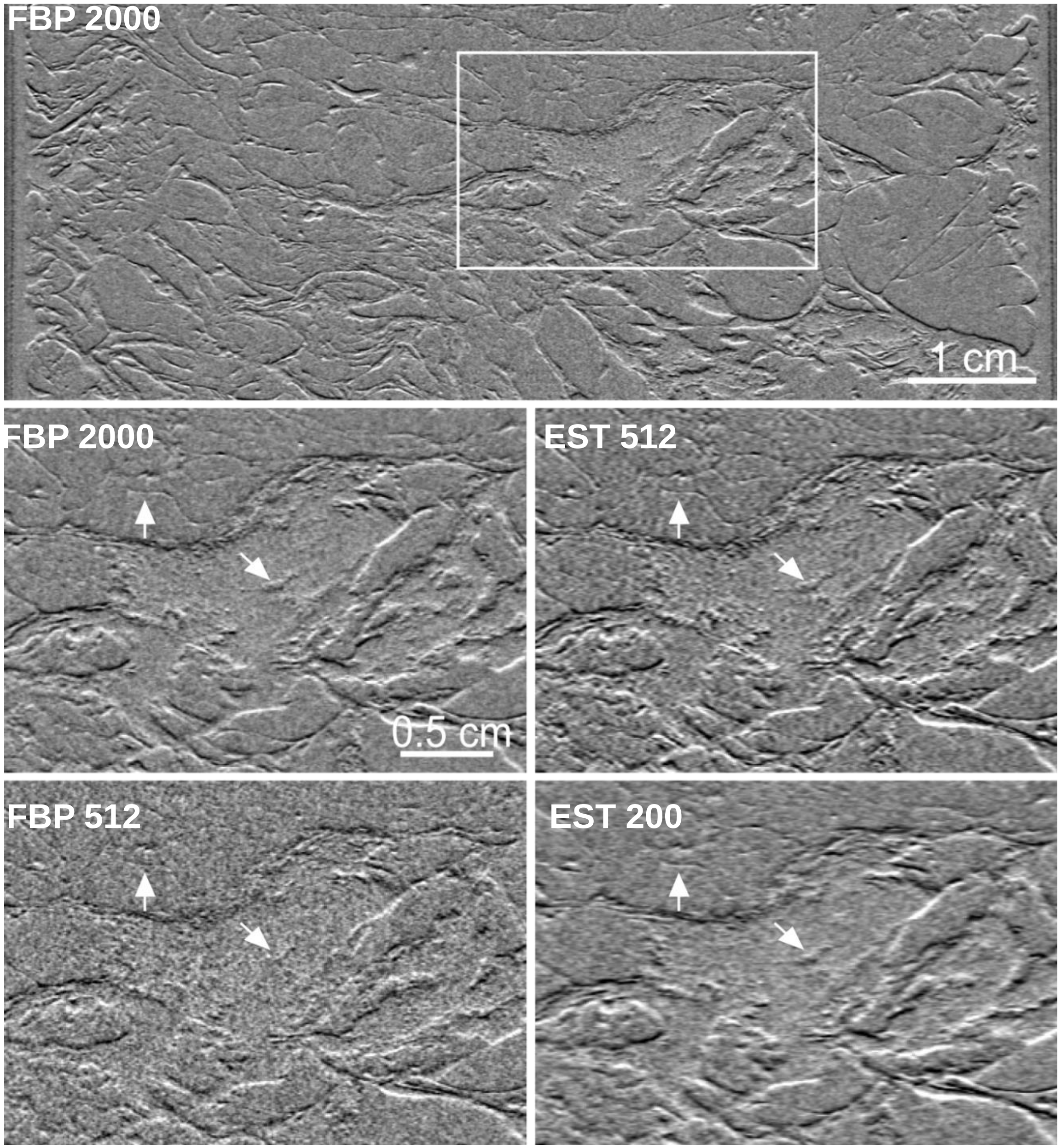

Identification of Detailed Features in the Breast Cancer Sample (EST 512)

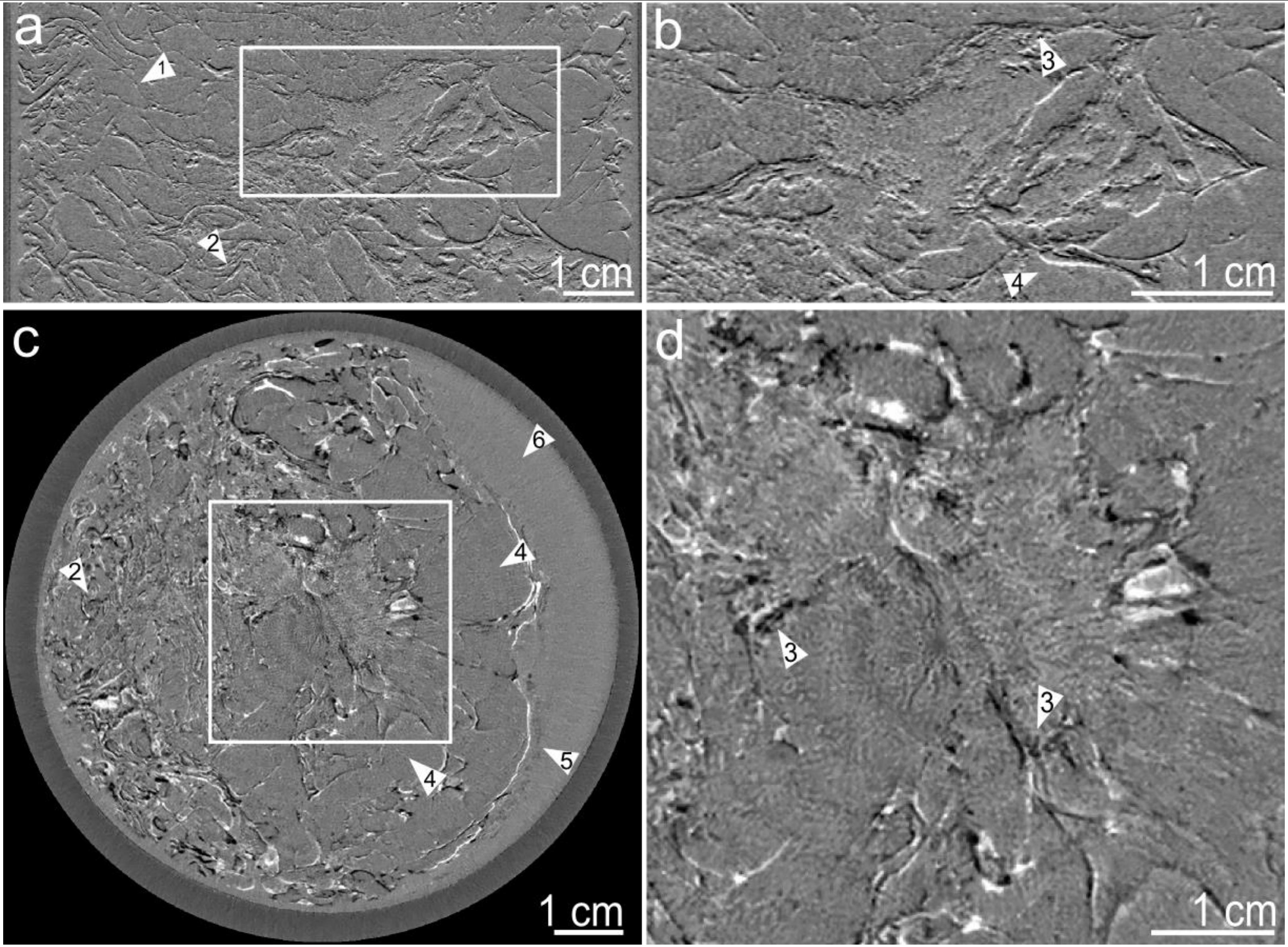

1) collagen strands; 2) glandular tissue; 3) spiculations; 4) fat; 5) skin; and 6) formalin

Blind Evaluation by Five Independent, Experienced Radiologists in Germany

	WBP (full)	EST (74% less dose)	WBP (74% less dose)	EST (90% less dose)
Overall image quality	4.3 ± 0.9	4.5 ± 0.5	2.2 ± 0.4	2.7 ± 0.9
Sharpness	4.0 ± 0.7	4.3 ± 0.5	3.3 ± 0.5	2.2 ± 0.8
Image contrast	4.0 ± 0.5	4.8 ± 0.4	3.0 ± 0.7	3.4 ± 1.0
Evaluation of different structure	4.1 ± 0.6	4.8 ± 0.4	2.6 ± 0.5	2.9 ± 1.0
Noise level	4.2 ± 0.6	4.8 ± 0.3	1.8 ± 0.8	3.3 ± 0.8

"5" - the best and "1" - the worst

Low-Dose 3D Diagnosis of Human Breast Cancers in Combination of Phase-Contrast X-ray Imaging and EST

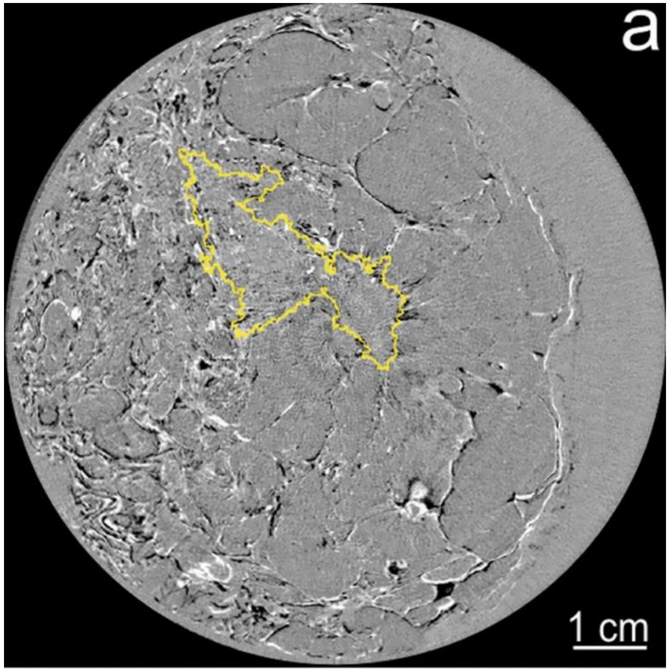

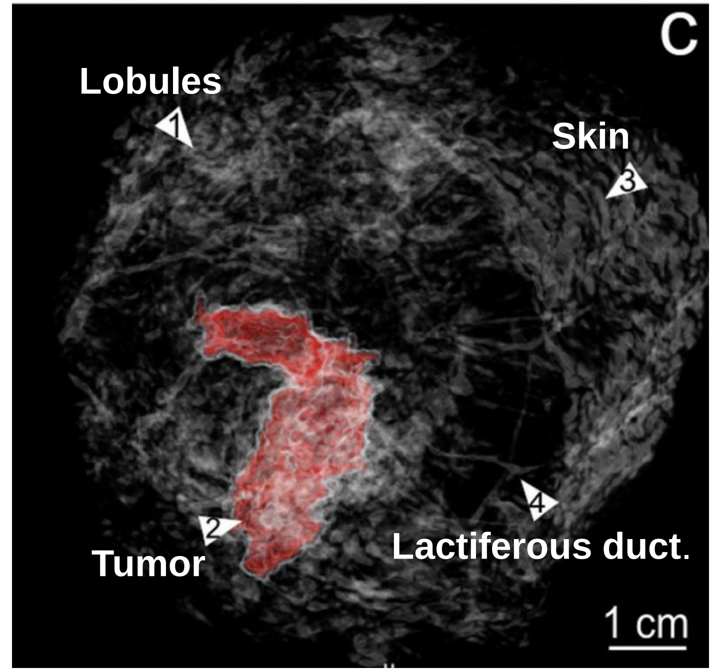

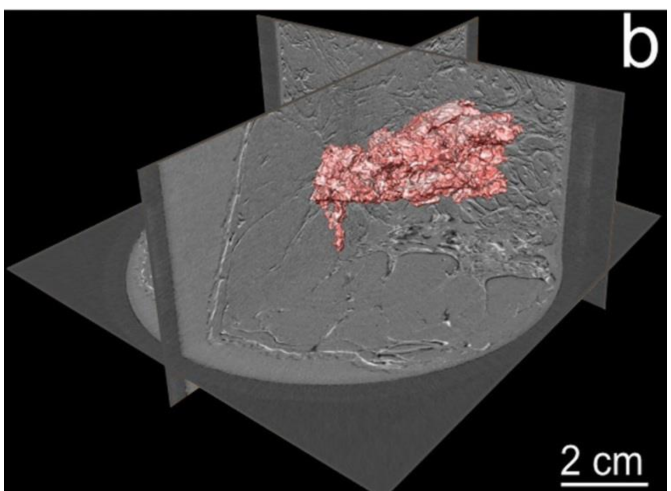

Mean Glandular Dose (MGD) for EST 512:
1.96 mGy

MGD for dual view clinical mammography:
3.4 mGy

Zhao, Brun, Coan, Huang, Sztrókay, Diemoz, Liebhardt, Mittone, Gasilov, Miao, Bravin, *PNAS* **109**, 18290–18294 (2012).

Summary

- A CM method has been developed to align tomographic projections at atomic precision.
- EST has been developed for the 3D tomographic reconstruction from a limited number of projections with a missing wedge.
- A general electron tomography method is achieved at 2.4 Å resolution; major grains are identified inside an icosahedral multiply twinned Au nanoparticle in three dimensions.
- Atomic steps at 3D twin boundaries and the 3D core structure of edge and screw dislocations are observed in a decahedral multiply twinned Pt nanoparticle at atomic resolution.
- The 3D coordinates of thousands of individual atoms and a point defect in a material are determined with ~19 pm precision; the 3D atomic displacement field and the full strain tensor are measured.
- We expect atomic resolution electron tomography to find broad applications in materials science, nanoscience, physics, chemistry and biology.

Collaborators

The Miao group at UCLA	*Mary Scott, Chien-Chun Chen, Rui Xu, Jose Rodriguez, Cun Zhu, Li Wu, Matthias Bartels, Yongsoo Yang, Jihan Zhou, AJ Pryor, Marcus Gallagher-Jones, Zhifeng Huang & Edwin Lee*
NCEM, LBNL	*Peter Ercius, Uli Dahmen, Colin Ophus & Jim Ciston*
UCLA	*Yu Huang, Chris Regan & Michael Sawaya*
Northwestern University	*Laurence Marks*
University of Birmingham	*Wolfgang Theis*
Stanford University	*Benjamin Fahimian*
ESRF	*Emmanuel Brun & Alberto Bravin*
University of Akron	*Hendrik Heinz & Hadi Ramezani-Dakhel*
Ludwig Maximilians Univ.	*Paola Coan*
Caltech	*Grant Jensen*
EMBL	*Daniel Castaño-Díez*

Supported by DOE, DARPA, NSF and ONR

Free software, codes and data sets: www.physics.ucla.edu/research/imaging